Revisiting the Relationship between Atlantic Dust and Tropical Cyclone Activity using Aerosol Optical Depth Reanalyses: 2003-2018

Peng Xian[1a], Philip J. Klotzbach[2a], Jason P. Dunion[3], Matthew A. Janiga[1], Jeffrey S. Reid[1] , Peter R. Colarco[4] and Zak Kipling[5]

[1]Naval Research Laboratory, Monterey, CA, USA.
[2]Department of Atmospheric Science, Colorado State University, Fort Collins, CO, USA.
[3]University of Miami/RSMAS/CIMAS – NOAA/AOML/Hurricane Research Division, Miami, FL, USA.
[4]NASA Goddard Space Flight Center, Greenbelt, MD, USA.
[5]European Centre for Medium-Range Weather Forecasts, Reading, UK.

[a] Peng Xian and Philip J. Klotzbach are joint-lead coauthors.
Correspondence: Peng Xian (peng.xian@nrlmry.navy.mil)

2
3
4
5
6
7
8
9
10
11
12
13
14
15
16
17
18
19
20
21
22
23
24
25
26
27
28
29
30
31
32
33

Abstract

Previous studies have noted a relationship between African dust and Atlantic tropical cyclone (TC) activity. However, due to the limitations of past dust analyses, the strength of this relationship remains uncertain. The emergence of aerosol reanalyses, including the Navy Aerosol Analysis and Prediction System (NAAPS) Aerosol Optical Depth (AOD) reanalysis, NASA Modern-Era Retrospective analysis for Research and Applications, Version-2 (MERRA-2) and ECMWF Copernicus Atmosphere Monitoring Service reanalysis (CAMSRA) enable an investigation of the relationship between African dust and TC activity over the tropical Atlantic and Caribbean in a consistent temporal and spatial manner for 2003-2018. Although June-July-August (JJA) 550 nm dust AOD (DAOD) from all three reanalysis products correlate significantly over the tropical Atlantic and Caribbean, the difference in DAOD magnitude between products can be as large as 60% over the Caribbean and 20% over the tropical North Atlantic. Based on the three individual reanalyses, we have created an aerosol multi-reanalysis-consensus (MRC). The MRC presents overall better root mean square error over the tropical Atlantic and Caribbean compared to individual reanalyses when verified with ground-based AErosol RObotic NETwork (AERONET) AOD measurements. Each of the three individual reanalyses and the MRC have significant negative correlations between JJA Caribbean DAOD and seasonal Atlantic Accumulated Cyclone Energy (ACE), while the correlation between JJA tropical North Atlantic DAOD and seasonal ACE is weaker. Possible reasons for this regional difference are provided. A composite analysis of three high versus three low JJA Caribbean DAOD years reveals large differences in overall Atlantic TC activity. We also show that JJA Caribbean DAOD is significantly correlated with large-scale fields associated with variability in interannual Atlantic TC activity including zonal wind shear, mid-level moisture and SST, as well as ENSO and the Atlantic Meridional Mode (AMM), implying confounding effects of these factors on the dust-TC relationship. We find that seasonal Atlantic DAOD and the AMM, the leading mode of coupled Atlantic variability, are inversely related and intertwined in the dust-TC relationship. Overall, DAOD in both the tropical Atlantic and Caribbean is negatively correlated with Atlantic hurricane frequency and intensity, with stronger correlations in the Caribbean than farther east in the tropical North Atlantic.

1. Introduction

Saharan dust particles can affect weather and climate through both direct and indirect radiative and cloud processes, notably in association with boreal summer Saharan Air Layer (SAL) outbreaks. The SAL is a layer of hot and dry air that forms over continental West Africa and is then advected over the low-level moist marine boundary layer of the tropical Atlantic (Carlson and Prospero, 1972). The SAL is often associated with the African Easterly Jet (AEJ) that can enhance vertical wind shear. Despite numerous observational and modeling studies that have examined the relationships between these aspects of the SAL and Atlantic TC activity, there are conflicting findings as to whether dust acts to generally inhibit or enhance tropical cyclogenesis and intensification. Some studies suggest negative impacts of the SAL's dust-laden dry air and the AEJ on TC activity (e.g., Dunion and Velden 2004; Lau and Kim 2007; Jones et al. 2007; Sun et al. 2008; Pratt and Evans 2008) while others have focused exclusively on the dust particles themselves and have found a negative influence on TCs (e.g., Evan et al. 2006a; Rosenfield et al. 2007; Strong et al. 2018; Reed et al. 2019). Other studies have suggested little impact of the SAL on TCs (e.g., Braun 2010; Sippel et al. 2011; Braun et al. 2013), while others have posited a positive impact of dust on TCs through cloud-microphysical processes (e.g., Jenkins et al. 2008). Finally, others have suggested that there are contrasting influences through different mechanisms and for different TCs (Karyampudi and Pierce, 2002; Bretl et al. 2015; Pan et al., 2018), highlighting the complexity of the dust-TC interaction.

African dust impacts the North Atlantic throughout the year, with its summer peak season (May-August) overlapping and leading the peak of the Atlantic hurricane season (August-October; Figure S1). As African dust outbreaks during the summer are often associated with the SAL, airborne dust has often been used as an indicator for the SAL (Dunion and Velden, 2004; Dunion, 2011; Tsamalis et al., 2013), although early season cases where the majority of the dust existed in the marine boundary layer below the trade wind inversion instead of staying aloft were also found (Reid et al., 2003). Saharan dust and the SAL are frequently observed throughout the Caribbean and as far west as Central America and the North American continent during the boreal summer (e.g., Prospero, 1999; Reid et al., 2003; Dunion and Velden 2004; Nowottnick et al., 2011; Kuciauskas et al., 2018). Airborne dust associated with the SAL often extends to 5.5 km (500 hPa) off of western Africa, and becomes thinner as its top lowers and its base rises as it is advected westward, shrinking to below 2 km in the Caribbean and in the Gulf of Mexico (Tsamalis et al., 2013). In some strong SAL cases, however, the top of the dust layer can reach 6 km (Reid et al., 2003; Colarco et al., 2003). During their trans-Atlantic transport, dust aerosols are from time to time observed to interact with TCs, as seen in satellite imagery (Figure 1).

African dust and its associated SAL has been hypothesized to impact TCs through a variety of mechanisms. Through scattering and absorbing sunlight, dust reduces solar radiation reaching the surface, thus cooling SSTs (e.g., Miller and Tegen, 1998; Lau and Kim 2007; Evan et al., 2009). Lower SSTs provide TCs with less energy to initiate, develop, and maintain strength. Through additional radiative heating of the dusty layer, mineral dust is also suggested to impact the structure, location and energetics of the AEJ (Tompkins et al., 2005; Wilcox et al., 2010; Reale et al., 2011) and African easterly wave (AEW) activity (Karyampudi and Carlson, 1988; Reale et al., 2009; Nathan et al., 2017; Jones et al., 2004; Ma et al., 2012; Grogan et al., 2016, 2017; Bercos-Hickey et al., 2017), thus having implications for tropical cyclogenesis. From a thermodynamic point of view, Dunion and Velden (2004) have proposed that the dust-carrying

109 SAL outbreaks could inhibit TC formation and development in the North Atlantic through three
110 primary mechanisms, including dry air intrusion into the storm, enhancement of the local vertical
111 wind shear associated with the enhanced AEJ, and stabilization of the environment due to
112 radiative heating of the dust layer above the marine boundary layer.

113 Dust particles can also act as cloud condensation nuclei (Twohy et al., 2009; Karydis et al.,
114 2011) and ice nuclei (DeMott et al., 2003; Sassen et al., 2003) and affect cloud microphysics,
115 weakening or strengthening convection depending on the environment (Khain, 2009). Focusing
116 specifically on TCs, there is not a consistent conclusion among studies on whether the
117 microphysical impacts of dust weaken or strengthen TCs (Jenkins et al., 2008; Rosenfeld et al.,
118 2007; Zhang et al., 2007, 2009; Herbener et al., 2014; Nowottnick et al., 2018).

119 While dust aerosols can affect TC formation and development through radiative and cloud-
120 microphysical impacts, TCs can in turn impact dust aerosol spatial distributions through wet
121 removal and dynamic flow (Herbener et al., 2016). AEWs, serving as seeding disturbances for
122 TCs (Landsea, 1993), are shown to contribute to dust emission and transport (e.g., Westphal et
123 al., 1987; Jones et al., 2003; Knippertz and Todd, 2010). Climate variability that affects TC
124 activity can also impact African dust emission and transport over the North Atlantic and
125 Caribbean. For example, ENSO was found to affect the emission and transport of African dust as
126 well (Prospero and Lamb, 2003; DeFlorio et al., 2016), especially during the boreal winter
127 (Prospero and Nees, 1986; Evan et al., 2006b).

128 How all of these factors interact in the complex climate system and to what extent they can
129 impact TC formation and intensification is still largely unknown. The goal of this study is to
130 explore how the integrated interactions manifest themselves in the relationship between Saharan
131 dust and Atlantic TC activity on seasonal to interannual time scales using state-of-the-art aerosol
132 reanalysis data. This serves as a first step towards further understanding the dust-TC relationship
133 and evaluating the relative importance of different mechanisms. Previous empirical studies on
134 the relationship between African dust and Atlantic TC activity are limited by uneven spatial and
135 temporal sampling by satellite and in situ-based observations. The emergence of several aerosol
136 reanalysis datasets, including the Navy Aerosol Analysis and Prediction System (NAAPS)
137 Aerosol Optical Depth (AOD) reanalysis (NAAPS-RA, Lynch et al., 2016), the Modern-Era
138 Retrospective analysis for Research and Applications, Version 2 (MERRA-2) aerosol reanalysis
139 (Randles et al., 2017) and the Copernicus Atmosphere Monitoring Service ReAnalysis
140 (CAMSRA) (Inness et al., 2019) allow us to investigate this relationship in a more consistent
141 manner over their joint time period to provide a degree of statistical robustness.

142 In section 2, an introduction to the aerosol and large-scale environmental data and the analysis
143 methods employed is provided. Section 3 presents the DAOD climatology, its interannual
144 variability over the Atlantic, and comparisons of the three aerosol reanalyses. This section also
145 evaluates correlations between DAOD and Atlantic TC activity, as well as the relationship
146 between DAOD and large-scale environmental conditions and climate modes. The sensitivity of
147 the results to the definition of the regions, the number of composite years used, and the definition
148 of dust seasons are provided in section 4. A discussion and conclusions are given in section 5.

149 **2. Data and Methods**

150 **2.1 Methods**

151 Regardless of the underlying mechanisms, as there are contradicting mechanisms proposed in
152 different studies, the goal of this study is to examine if there is a robust and statistically
153 significant relationship between African dust and Atlantic TC activity on seasonal to interannual
154 time scales. We also examine if there are confounding factors, for example, meteorological
155 conditions and climate modes that co-vary with dust and hence influence TC activity.

156 We use dust AOD (DAOD) to represent Atlantic dust levels. Three aerosol reanalysis products,
157 and their consensus DAOD are used in order to increase the fidelity of the analysis result, given
158 that multi-model-consensus typically has been shown to have better data quality in prior
159 assessments (Sessions et al., 2015; Xian et al., 2019). Various TC count indices and
160 Accumulated Cyclone Energy (ACE) (Bell et al. 2000), defined in the next section, are utilized
161 to represent TC activity.

162 The Atlantic Main Development Region (MDR) (e.g., Goldenberg et al., 2001), including the
163 Caribbean (10-20°N, 85-60°W) and the tropical North Atlantic (10-20°N, 60-20°W), are the
164 focus regions for this study (see also Figure 2 for a spatial representation of the two subregions).
165 Most previous studies of dust impacts on TC activity have focused on the tropical North Atlantic
166 or regions closer to the African continent (e.g., Karyampudi and Pierce, 2002; Bretl et al. 2015;
167 Pan et al., 2018) where DAOD is relatively high. However significant dust pulses can also be
168 transported into the Caribbean. We therefore expand our study area to explore the potential
169 impacts of high levels of dust in the Caribbean on Atlantic TC activity. This allows us to explore
170 regional differences in the dust-TC relationship. Statistical relationships between DAOD and TC
171 activity over the MDR are investigated using the three aerosol reanalyses and multi-reanalysis-
172 consensus (MRC). The results obtained herein also help us assess the potential of using DAOD
173 to aid in future Atlantic seasonal hurricane forecasts.

174 The correlations between variables of interest are based on the Pearson correlation coefficient.
175 Statistical significance is assessed at the 95% level using a two-tailed Student's t-test.
176 Correlations $>= 0.51$ are statistically significant given that a 16-year time period (e.g., 2003-
177 2018) is investigated here. For partial correlation analysis, partial correlations $>=0.55$ are
178 statistically significant at the 95% level with 13 degrees of freedom. The criteria for statistical
179 significance with various degrees of freedom can also be obtained at:
180 https://www.esrl.noaa.gov/psd/data/correlation/significance.html.

2.2 Aerosol data

182 A combination of aerosol reanalyses are used to describe the aerosol environment over the
183 tropical North Atlantic and Caribbean. An aerosol multi-reanalysis-consensus (MRC) based on
184 three aerosol reanalysis products, including the NAAPS-RA (Lynch et al., 2016) from the US
185 Naval Research Laboratory, MERRA-2 (Randles et al., 2017) from NASA, and CAMSRA
186 (Inness et al., 2019) from ECMWF, are also generated and used. The analysis period is focused
187 on 2003-2018, when all three aerosol reanalyses are available and both Terra and Aqua Moderate
188 Resolution Imaging Spectroradiometer (MODIS) AOD retrievals were assimilated therein.

2.2.1 NAAPS AOD reanalysis

190 The NAAPS-RA product provides 550 nm speciated AOD at a global scale with 1°x1° degree
191 spatial and 6-hourly temporal resolution for the years 2003-2018 (Lynch et al., 2016). This

192 reanalysis uses a modified version of NAAPS and assimilates quality-controlled AOD retrievals
193 from MODIS on Terra and Aqua and the Multi-angle Imaging SpectroRadiometer (MISR) on
194 Terra (Zhang et al., 2006; Hyer et al., 2011; Shi et al., 2011). NAAPS characterizes
195 anthropogenic and biogenic fine aerosol species (ABF), dust, sea salt and biomass burning
196 smoke aerosols. The aerosol source functions were tuned regionally so that a best match between
197 the model coarse and fine mode AODs and the Aerosol Robotic Network (AERONET) AODs
198 can be obtained. Other model processes, e.g. deposition, were also tuned to minimize the AOD
199 difference between the model and quality-controlled satellite AOD retrievals. NOAA Climate
200 Prediction Center MORPHing (CMORPH) precipitation derived from satellite observations
201 (Joyce et al., 2004) is used to correct precipitation biases in the tropics for better AOD analyses
202 through wet deposition processes (Xian et al., 2009). The reanalysis captures the decadal AOD
203 trends detected using standalone satellite products in other studies (e.g., Hsu et al., 2012; Zhang
204 et al., 2017), demonstrating the quality of the reanalysis product for climate studies. The
205 NAAPS-RA data for May 2017 - November 2018 was generated by assimilating MODIS DA-
206 quality AOD only without MISR AOD assimilation because of the unavailability of MISR DA-
207 quality data at the time of this study. The impact of not including MISR is expected to be minor
208 as MISR provides only about 10% of the total assimilated AOD data. Additionally, differences
209 between monthly mean DA-quality AOD over the MDR region derived using both MODIS and
210 MISR versus using only MODIS were found to be negligible (not shown).

211 **2.2.2   MERRA-2 AOD reanalysis**

212 As part of the upgrade from the original MERRA reanalysis (Rienecker et al., 2011) based on the
213 Goddard Earth Observing System (GEOS) Earth system model, MERRA-2 now incorporates
214 assimilation of AOD from a variety of remote sensing sources, including AERONET, MODIS,
215 and MISR after 2000, and AVHRR before 2002. The aerosol module used for MERRA-2 is the
216 Goddard Chemistry, Aerosol, Radiation, and Transport model (GOCART; Chin et al. 2000;
217 Colarco et al., 2010), which provides simulations of dust, sea salt, black and organic carbon, and
218 sulfate aerosols, and is run radiatively coupled to the GEOS AGCM. A detailed description and
219 validation of the AOD reanalysis product can be found in Randles et al. (2017) and Buchard et
220 al. (2017). For the purpose of this study, monthly mean DAOD at 550 nm with 0.5° latitude and
221 0.625° longitude spatial resolution is used. MERRA-2's longer data record (1981-present)
222 would have made it an ideal candidate for a longer-period analysis of the relationship between
223 DAOD and TCs. However, the volcanic eruptions of El Chichon (1982) and Pinatubo (1991)
224 result in high AOD for several years following each event, and the particle property assumptions
225 in MERRA-2 do not properly apportion the assimilated AOD increments among the simulated
226 aerosol species. For the 2003-2018 time period, MERRA-2 AOD data has similar validation
227 statistics compared to NAAPS-RA and CAMSRA at the sites located off of the coast of West
228 Africa and the Caribbean, as shown in Table 1.

229 **2.2.3 CAMSRA AOD reanalysis**

230 Under the banner of the Copernicus Atmosphere Monitoring Service (CAMS), operated by
231 ECMWF on behalf of the European Commission, a new global reanalysis of atmospheric
232 composition has been produced: CAMSRA (Inness et al., 2019). This is the successor to the
233 MACC reanalysis (Inness et al., 2013) and CAMS interim reanalysis (Flemming et al., 2017)
234 produced previously at ECMWF. The dataset spans the period 2003–2018 and is being continued
235 for subsequent years. The model component is based on the same Integrated Forecasting System

236 (IFS) used at ECMWF for weather forecasting and meteorological reanalysis, but at a coarser
237 resolution and with additional modules activated for prognostic aerosol species (dust, sea salt,
238 organic matter, black carbon and sulphate) and trace gases. The impact of the aerosols (and
239 ozone) on radiation and thereby on meteorology is included in the model. For aerosol,
240 observations of total AOD at 550nm are assimilated from MODIS (Terra and Aqua) for the
241 whole period, and from the Advanced Along-Track Scanning Radiometer for 2003–2012, using a
242 4D variational data assimilation system with a 12-hour data assimilation window along with
243 meteorological and trace gas observations. The speciated AOD products used in this study are
244 available at a 3-hourly temporal resolution and a ~0.7° spatial resolution. Model development
245 has generally improved the speciation of aerosols compared with earlier reanalyses, and
246 evaluation against AERONET is largely consistent over the period of the reanalysis. There is a
247 known issue regarding a significant overestimation of sulfate near outgassing volcanoes;
248 however this is unlikely to have much relevance to the regions considered in this study.

249 **2.2.4 AOD multi-reanalysis-consensus (MRC)**

250 Based on the three aerosol reanalysis products described above, we made a MRC product
251 following the multi-model-ensemble method of the International Cooperative for Aerosol
252 Prediction (ICAP, Sessions et al., 2015; Xian et al., 2019). The MRC is a consensus mean of the
253 three individual reanalyses, with a 1°x1° degree spatial and monthly temporal resolution.
254 Speciated AODs and total AOD at 550nm for 2003-2018 are available. This new product is
255 validated with ground-based AERONET observations for African-dust-influenced regions,
256 including the western coast of North Africa and the Caribbean Sea. Validation results in terms of
257 RMSE for total and coarse-mode AODs are presented in Table 1. Similar to the ICAP multi-
258 model-ensemble evaluation result, the MRC is found to generally be the top performer among all
259 of the reanalyses for the study region.

260 **2.2.5 AErosol RObotic NETwork (AERONET) fine and coarse mode AOD**

261 AERONET is a ground-based global scale sun photometer network that includes instruments to
262 measure sun and sky radiance at wavelengths ranging from the near ultraviolet to the near
263 infrared during daytime hours. This network has been providing high-accuracy and high-quality
264 measurements of aerosol properties since the 1990s (Holben et al., 1998; Holben et al., 2001)
265 and is often used as the primary dataset for validating aerosol optical properties in satellite
266 retrievals and model simulations (e.g., Levy et al., 2010; Colarco et al., 2010; Kahn and Gaitley,
267 2015). Only cloud-screened, quality-assured version 3 Level 2 AERONET data are utilized in
268 this study (Giles et al., 2019). AERONET multiple wavelength measurements were used to
269 derive both fine and coarse mode AODs at 550 nm based on the Spectral Deconvolution Method
270 (SDA) of O'Neill et al. (2003). The SDA product was verified with in situ measurements (Kaku
271 et al., 2014) and was shown to be able to capture the full modal properties of fine and coarse
272 particles. Temporally, AERONET data are averaged into 6-hr bins centered at the regular model
273 output times of 0, 6, 12 and 18 UTC. Monthly mean AERONET AOD is derived only when the
274 total number of 6-hr AERONET data is greater than 18 to ensure temporal representativeness.

275 **2.3 Tropical Cyclone data – HURDAT2**

276 Atlantic basin TC data were taken from the Atlantic hurricane database version 2 (HURDAT2;
277 Landsea and Franklin, 2013). This dataset contains six-hourly information (including position,

maximum sustained winds, and central pressure – where available) for every TC observed in the Atlantic basin dating back to 1851.

2.4 Atmospheric data - ERA-Interim Reanalysis

The ERA-Interim Reanalysis (Dee et al., 2011) is a global atmospheric reanalysis produced by the ECMWF that uses a 4-dimensional variational analysis with a 12-hour analysis window. The spectral resolution of this data is approximately 80 km (T255) and is available on 60 vertical levels from the surface to 0.1 hPa and is available from January 1979 – August 2019. We use monthly mean large-scale fields, including vector wind, atmospheric temperature and relative humidity data on several pressure levels.

2.5 Oceanic data - NOAA OI SST

The National Oceanic and Atmospheric Administration (NOAA) Optimum Interpolation (OI) SST product (Reynolds et al., 2002) is utilized for SST calculations. NOAA OI SST v2 uses a combination of in-situ data, satellite data, SSTs simulated by sea-ice cover, and bias adjustments to arrive at its final estimate of SSTs. NOAA OI SST V2 data is available on a 1° x 1° grid from November 1981-present.

2.6 Climate indices

The Oceanic Nino Index (ONI), defined to be a three-month average of the Niño 3.4 (5°S-5°N, 170-120°W) index (Barnston et al., 1997) based on centered 30-year periods which are updated every five years, is utilized to represent the state of El Niño-Southern Oscillation (ENSO). This index is also used by NOAA to identify ENSO events.

The SST component of the AMM (Kossin and Vimont, 2007) is investigated to assess the relationship between DAOD and tropical Atlantic oceanic conditions. While the index is not standardized, we have standardized it by its 1981-2010 average and standard deviation.

2.7 Derived tropical cyclone indices

The genesis potential index (GPI) was calculated using monthly-averaged ERA-Interim data following Emanuel and Nolan (2004). The maximum potential intensity (MPI) was calculated using monthly-averaged ERA-Interim temperature and moisture and NOAA OI SST following Bister and Emanuel (2002).

3. Results

3.1 Dust aerosol optical depth over the MDR (2003-2018)

Figure 2 shows the MRC monthly DAOD climatology based on the 2003-2018 average as well as the ratio of DAOD to total AOD for June-October over the tropical Atlantic. Climatologically from June-October, the majority of airborne dust originates from the Sahara Desert, in contrast to the winter season when a significant amount of dust is emitted over the Sahel and southern Sahara (Engelstaedter and Washington, 2007). This dust is then transported westward over the Atlantic and eventually to the Caribbean, largely within the 10-25°N latitude belt. The transported African dust covers most of the Atlantic hurricane MDR, which spans the tropical North Atlantic and Caribbean. The DAOD over the Atlantic is, on average, much higher in June,

July, and August (JJA) than in September and October because of higher emissions over the African continent in the former months (Carlson and Prospero 1972; Engelstaedter and Washington, 2007; Dunion and Marron, 2008; Dunion, 2011). DAOD is also much higher over the tropical Atlantic than over the Caribbean, as dust aerosols are removed by wet and dry processes during the long-range transport. The MRC shows that dust aerosols are the dominant contributor to the total AOD in the MDR during most of the hurricane season (June-October). The DAOD accounts for about 50-60% of the total AOD over the tropical North Atlantic and around 30-50% over the Caribbean for JJA. This suggests that the total AOD can be a relatively good indicator of DAOD in the tropical North Atlantic but is not as good of an indicator in the Caribbean for JJA. The DAOD contribution to total AOD is about 10-20% less for September and October. Considering the potential larger forcing by airborne dust in JJA than in September and October, the focus season in this study is JJA.

As transport of Saharan dust across the Atlantic during summer is often associated with SAL outbreaks, which are approximately centered around 700 hPa (Dunion and Velden, 2004; Dunion, 2011), monthly climatological 700 hPa relative humidity (RH) and horizontal wind are also shown in Figure 2. Climatologically, the MDR is dominated by the mid-level easterly jet (7-8 m s^{-1}) during JJA and weaker easterlies (5-6 m s^{-1}) during September and October. Over the Caribbean, the wind direction veers slightly towards the north for all of the studied months and relates to this region being typically positioned on the west side of the climatological Atlantic subtropical ridge. 700 hPa RH is on the order of 40% and 50% for the tropical Atlantic and the Caribbean respectively for JJA and is about 10% higher in September and October. RH is higher in the Caribbean than in the tropical North Atlantic as the impact of dry air from the SAL and from upper-level subsidence becomes weaker from east to west. For context, the Atlantic moist tropical sounding, defined in Dunion (2011), has average 700 hPa winds of 3.6 m s^{-1} at 112° (wind direction) and 66% RH, while the mean SAL sounding has corresponding values of 7.8 m s^{-1} at 91° and 34% RH.

Figure 3 shows the monthly mean AERONET version 3 L2 and MRC 550 nm modal AOD time series at four AERONET sites that are primarily influenced by African dust. From east to west, these sites include Dakar, Senegal (14.4°N, 17.0°W), Cape Verde (16.7°N, 22.9°W), Ragged Point, Barbados (13.2°N, 59.4°W), and La Parguera, Puerto Rico (18.0°N, 67.0°W), which are also marked in Figure 1. The boreal summer peak dust activity (i.e., JJA) is highlighted. Dust aerosols are typically considered coarse-mode, although there may be a very small amount of mass in fine-mode. The fine-mode AOD observed in AERONET measurements for these sites are normally dominated by pollution and biomass-burning smoke. Dakar and Cape Verde experience dust aerosols throughout the year, with a peak in JJA and a weaker secondary peak during the boreal winter, which is associated with dust emissions from the Sahel. The Ragged Point and La Parguera sites, which are remote receptor sites in the Caribbean, are influenced by African dust predominantly during boreal summer, thus displaying a pronounced peak of total and coarse-mode AODs in JJA. The secondary AOD peak during winter at Dakar and Cape Verde is generally not observed at Ragged Point or La Parguera, as African dust is transported to the south following the low-to-mid-level trade wind flow, occasionally reaching South America (Prospero, 2014).

Figure 3 also shows the bias, the root mean square error (RMSE) of MRC and the correlation (*r*) between MRC and AERONET for monthly AODs at each of the four AERONET sites. Overall,

MRC follows the seasonal and interannual variability in AERONET data for the total AOD quite well, and to a slightly lesser extent for the coarse-mode AOD. Coarse-mode aerosols include dust and sea salt, but are dominated by dust aerosols over the tropical North Atlantic for JJA (Figure 2c, speciated AOD cannot be obtained from AERONET measurements). The correlation is >~0.9 for the coarse-mode AOD and tends to be better at the long-range transport sites (i.e., Ragged Point and La Parguera) than the sites close to the dust source (i.e., Dakar and Cape Verde). The correlation is slightly lower in the source area than in the long-range transport region because there are large uncertainties in emissions and strong gradients due to local aerosol sources in the source area. Also, the source area allows less time for AOD data assimilation to correct aerosol mass loads, in addition to a lower signal/noise ratio of AOD retrievals over land than over water (e.g., Levy et al., 2005). The small bias, low RMSE and the high correlation with AERONET data illustrate the ability of MRC to capture the aerosol environment in the MDR. In addition, all of the three individual aerosol reanalyses that form the foundation of MRC have similar verification scores against AERONET, though the MRC typically has a better verification score than the individual reanalyses (Table 1). If we were to give different qualitative ratings for the three individual reanalyses for the study area, MERRA-2 is slightly better over North Africa and NAAPS-RA is slightly better over the Caribbean in terms of coarse-mode and total AOD RMSEs.

Figure 4 shows the time series of monthly mean and regionally-averaged DAOD from MRC and the three contributing reanalyses from 2003-2018 for the tropical North Atlantic and Caribbean as defined in Fig. 2. The DAODs from the three reanalyses have similar seasonal and interannual variability and are highly correlated, with $r >= 0.95$ for the entire 16-yr period and $r >= 0.85$ for JJA for both regions based on monthly means. The magnitudes of JJA DAOD from the three individual reanalyses are comparable over the tropical North Atlantic, with a 20% maximum difference among the three products based on JJA DAOD. The climatological average of JJA DAOD over the tropical North Atlantic is 0.21. The difference can be as much as ~0.06 (a ~60% difference between member products) for the Caribbean. The climatological average of JJA DAOD in the Caribbean is 0.10. Since the total and coarse-mode AOD verification statistics for the three products at the Caribbean AERONET sites are similar (Table 1), the DAOD difference is most likely due to the different partitioning of aerosol species (e.g., dust versus sea salt aerosols) during the total AOD data assimilation process. This is related to the fact that total AOD is the only aerosol property constrained by satellite observations through AOD data assimilation in all three aerosol reanalysis products, while speciated AOD is not constrained (Lynch et al., 2016; Randles et al., 2017; Inness et al., 2019). Nevertheless, the DAOD from the MRC is likely the most reliable given the generally better performance of multi-aerosol model consensus compared to individual aerosol models (Sessions et al., 2015; Xian et al., 2019).

3.2 Relationship between North Atlantic TC activity and JJA DAOD

Accumulated Cyclone Energy (ACE) is often utilized to represent TC activity and is defined to be the square of the one-minute maximum sustained wind speed at each six-hourly interval when a tropical or subtropical cyclone (with maximum sustained winds >=34 kt) is present (Bell et al., 2000). Basin-wide ACE is used here, as it is assumed that MDR conditions affect to some extent, the ACE of all storms that pass through the MDR, including those that later moved out of the MDR. For example, we hypothesize that in an active dust year, the suppressed conditions in the MDR would make for weaker, less organized AEWs that have less of a chance for formation

404 even if they do eventually move out of the MDR. Later we show in Table 2 that using ACE
405 generated in the Caribbean domain yields a consistent (same sign) yet stronger correlation
406 relationship between DAOD and ACE.

407 Atlantic TC activity shows a statistically significant relationship with regionally-averaged
408 Caribbean JJA DAOD. Figure 5a displays this relationship, with higher Caribbean DAOD
409 correlating (r = -0.61 with MRC DAOD and r of similar magnitudes from all three individual
410 reanalyses and exceeding the two-tailed 95% statistical significance level) with quieter Atlantic
411 hurricane seasons as quantified by ACE. While tropical North Atlantic DAOD and Caribbean
412 DAOD in JJA correlate strongly (r = 0.88), Figure 5b shows that the relationship between
413 DAOD and ACE is weaker in the tropical North Atlantic than in the Caribbean. The correlation
414 between tropical North Atlantic DAOD and ACE is -0.41, which falls below the statistical
415 significance threshold (correlations with MERRA-2 and CAMSRA DAODs are also
416 insignificant). We will show in the next section that the relationship between large-scale fields
417 known to impact Atlantic TC activity also tend to have higher correlations with JJA Caribbean
418 DAOD than with JJA tropical North Atlantic DAOD.

419 Given the strength of the relationship between Caribbean DAOD and seasonal Atlantic ACE, we
420 next investigate the relationship in extreme JJA DAOD seasons. We take the three seasons from
421 2003-2018 when JJA Caribbean DAOD was at its highest levels and when it was at its lowest
422 levels.

423 The three seasons with the highest JJA Caribbean DAOD were 2018, 2015 and 2014 in
424 descending order, and the three seasons with the lowest JJA Caribbean DAOD were 2005, 2011
425 and 2017 in ascending order based on MRC. The left column of Figure 6 shows DAOD
426 composites for the three high and the three low JJA Caribbean DAOD seasons and their
427 differences. DAOD is not only higher over the MDR in the high Caribbean DAOD seasons, but
428 dust aerosols are transported farther to the west. DAOD differences between the extreme high
429 and low DAOD seasons over the tropical North Atlantic and Caribbean are ~0.05-0.08. In fact,
430 the three high dust years have roughly 60% more DAOD in the Caribbean than the three low
431 dust years (regional average of 0.13 vs. 0.08), while these differences are not as large in the
432 tropical North Atlantic. The transport pathway of dust is also shifted slightly to the south in the
433 tropical North Atlantic in the three high DAOD seasons.

434 The right column of Figure 6 displays the JJA-averaged 850 hPa winds and 700 hPa RH for the
435 three high and three low JJA Caribbean DAOD seasons, and the difference between these high
436 and low seasons. Large-scale conditions over the Caribbean during JJA were much less
437 conducive for TCs in the high DAOD seasons, with drier middle levels (>10% relative humidity
438 difference) and stronger easterly trade winds (2-4 m s^{-1} stronger), implying an overall less
439 hurricane-favorable dynamic and thermodynamic environment. This is consistent with the
440 depiction of the thermodynamic structure of the SAL by Dunion and Velden (2004). The
441 stronger AEJ associated with higher DAOD is also consistent with modeling studies when
442 aerosol radiative effects are taken into account (Tompkins et al., 2005). Associated with high
443 Caribbean DAOD, the position of the center of the Azores High was slightly shifted to the
444 southwest, which facilitates stronger dust transport into the Caribbean. This is in agreement with
445 the findings of Riemer and Doherty (2006) who suggested the importance of the position of the
446 Azores High in African dust transport across the Atlantic, although their study was only during

447 the boreal winter. As would be expected from these large-scale conditions, Atlantic TC activity
448 was much higher in low JJA Caribbean DAOD seasons.

449 Table 2 displays observed Atlantic TC activity as well as the ratios of observed average seasonal
450 Atlantic TC activity in the three low JJA Caribbean DAOD seasons versus the three high
451 Caribbean DAOD seasons. Atlantic basin-wide numbers of tropical depressions, named storms,
452 hurricanes, major (Category 3+ on the Saffir-Simpson Hurricane Wind Scale) hurricanes and
453 ACE are higher by a factor of ~1.9 - ~2.8 in the three low relative to the three high Caribbean
454 DAOD seasons. The ratios are even higher (e.g., 12 times higher for ACE) for TC activity in the
455 Caribbean. The 2018 Atlantic hurricane season was an interesting case, as it was an above-
456 average overall hurricane season (as measured by ACE), but much of the ACE that was
457 generated that year occurred outside of the tropics (>23.5°N) (Saunders et al. 2020). Very little
458 activity occurred in the Caribbean in 2018.

459 In addition, the ratio for major hurricanes is higher than the ratios for tropical depressions,
460 named storms, and hurricanes, indicating a stronger relationship between dust aerosols and
461 intense storms than between dust aerosols and weak storms. A total of 17 major hurricanes were
462 observed in the Atlantic in the three low Caribbean DAOD seasons, compared with only 6 major
463 hurricanes in the three high Caribbean DAOD seasons. The three low Caribbean DAOD seasons
464 had six continental United States major hurricane landfalls (2005 Hurricanes Dennis, Katrina,
465 Rita, and Wilma and 2017 Hurricanes Harvey and Irma), while the three high Caribbean DAOD
466 seasons had one continental United States major hurricane landfall (2018 Hurricane Michael).

467 Figure 7 displays the named storm formation location of all Atlantic TCs in the three seasons
468 with the highest JJA Caribbean DAOD and the three seasons with the lowest Caribbean DAOD
469 along with the maximum intensity that these TCs reached. As would be expected from the
470 differences in large-scale conditions noted earlier, TCs that became major hurricanes formed
471 much more frequently south of 20°N in the three lowest Caribbean DAOD seasons than in the
472 three highest Caribbean DAOD seasons. These differences were most pronounced in the
473 Caribbean, with only one named storm (Hanna in 2014) forming in the Caribbean in the three
474 highest JJA Caribbean DAOD seasons. In the three lowest Caribbean JJA DAOD seasons, 11
475 named storms formed in the Caribbean.

476 **3.3 Relationship between JJA DAOD and large-scale atmosphere/ocean fields**

477 We next examine the relationship between JJA DAOD and large-scale atmosphere/ocean fields.
478 In this analysis, we begin by focusing on several fields that have been documented in prior
479 research to significantly impact Atlantic TC activity: 850 hPa zonal wind (850 hPa U), 200 hPa
480 zonal wind (200 hPa U), zonal wind shear between 200 hPa and 850 hPa, 700 hPa RH, 850 hPa
481 relative vorticity and SST (Gray, 1968; Saunders et al., 2017). More active Atlantic hurricane
482 seasons are typically associated with anomalous westerly 850 hPa U (e.g., weaker trade winds),
483 anomalous easterly 200 hPa U (counteracting prevailing upper-level westerlies) and thus weaker
484 wind shear, higher 850 hPa relative vorticity, higher mid-level relative humidity and
485 anomalously warm SSTs. We investigate the relationships with DAOD in the tropical North
486 Atlantic and the Caribbean as defined in Figure 2.

487 Figure 8 displays the correlation between regionally-averaged MRC JJA DAOD in the Caribbean
488 and the six large-scale fields just discussed. Higher JJA Caribbean DAOD is associated with

489 stronger 850 hPa easterly trades and increased 200 hPa upper-level westerlies (and hence
490 stronger vertical wind shear), drier air at 700 hPa and anomalously cool SST across the MDR.
491 Weaker 850 hPa relative vorticity also predominates over most of the Caribbean. However,
492 almost no correlation is found between Caribbean JJA DAOD and 850 hPa relative vorticity in
493 the tropical North Atlantic, possibly due to the counteracting role of covariability of African dust
494 emissions and AEWs - as was inferred from a positive correlation between the two by
495 Karyampudi and Carlson (1988). This result is also consistent with Figure 7 which shows more
496 named storms and therefore likely stronger AEW activity right off of the coast of west Africa
497 between 10-20°N in high dust DAOD years. This result reflects the complexity of the TC-dust
498 interaction relationship. In addition, the vorticity field is extremely noisy. Figure 8f is extended
499 to include the eastern and central tropical Pacific in order to investigate the potential relationship
500 between ENSO and DAOD, with Caribbean DAOD showing a significant positive relationship
501 with ENSO.

502 The relationship between the same six large-scale fields and JJA tropical North Atlantic DAOD
503 is considerably weaker, with lower correlations observed for all six fields (Figures S2). In
504 addition, the regions with significant correlations decrease in spatial extent relative to the
505 Caribbean DAOD correlations shown in Figure 8.

506 We next investigate Maximum Potential Intensity (MPI), an integrated TC index, which
507 combines a list of key factors (similar to those explored above). MPI assesses how conducive
508 atmospheric thermodynamic conditions are for TC intensification, providing a theoretical limit of
509 the strength of a TC (Holland, 1997; Bister and Emanuel, 1998). Figures 9a and c show the
510 correlations between the Caribbean region-averaged JJA DAOD and JJA/ASO MPI calculated
511 based on Bister and Emanuel (1998). Consistent with the results for the individual large-scale
512 fields, JJA MPI over the MDR exhibits strong negative correlations with JJA Caribbean DAOD
513 (~ -0.7, also Table 3). One of the primary inputs to the MPI calculation is SST, so the strong
514 inverse relationship between MPI and DAOD is expected given the strong inverse relationship
515 between SST and DAOD. The correlation is significant but weaker for ASO MPI for most of the
516 MDR, except for the eastern tropical North Atlantic, where the negative correlation drops below
517 statistical significance. The negative correlation of JJA/ASO MPI with JJA tropical North
518 Atlantic region-averaged DAOD is much weaker than that with JJA Caribbean DAOD in the
519 MDR (Figure 9b and d) and drops below statistical significance in the Caribbean.

520 The genesis potential index (GPI) is another integrated TC index that is often used to provide an
521 estimate of the potential for tropical cyclogenesis (e.g., Emanuel and Nolan, 2004; Camargo et
522 al., 2007). Monthly GPI is calculated following Emanuel and Nolan (2004). Figure 10 shows the
523 correlation between region-averaged JJA DAODs and JJA and ASO GPI. Consistent with the
524 results for the individual large-scale fields and MPI, JJA GPI over the MDR exhibits strong
525 negative correlations (~-0.7, also Table 3) with JJA Caribbean DAOD. Similar to MPI, GPI is
526 also directly related to SST via the potential intensity term, so given the negative correlation
527 between DAOD and SST, we would expect a negative correlation between GPI and DAOD.
528 Other terms also comprise the GPI, including vertical wind shear and mid-level moisture, which
529 also correlate negatively with DAOD. The correlation remains statistically significant but is
530 weaker for ASO GPI for most of the MDR. The exception is the eastern tropical North Atlantic,
531 where the negative correlation drops below 95% statistical significance. The negative correlation
532 of JJA/ASO GPI with JJA tropical North Atlantic region-averaged DAOD is much weaker than

533 that with JJA Caribbean DAOD in the MDR (Figure 10b and d), which is also consistent with the
534 result for the individual large-scale fields and MPI.

535 Table 3 summarizes the relationship between large-scale atmosphere/ocean fields, MPI, GPI, and
536 DAOD, with correlations displayed between JJA region-averaged DAOD and concurrent region-
537 averaged fields (i.e., JJA-averaged), as well as the large-scale region-averaged fields during the
538 peak of the Atlantic hurricane season from August-October. 850 hPa relative vorticity is
539 excluded as no statistically significant correlations are found. While the correlations between the
540 other five large-scale fields, MPI, GPI, and DAOD tend to weaken from JJA to ASO, the
541 correlations remain significant for all of these large-scale fields, and the integrated TC indices, in
542 the Caribbean during ASO. For the tropical North Atlantic, JJA DAOD has much weaker and
543 insignificant correlations with JJA 200 hPa zonal wind, wind shear and 700 hPa RH compared to
544 those for the Caribbean. However its negative correlation with SST is as strong as that for the
545 Caribbean in JJA and remains statistically significant from JJA to ASO, although the magnitude
546 of the correlation is weaker in ASO. These contribute to a negative correlation with MPI and GPI
547 and a stronger correlation during JJA than during ASO.

548 Part of the reason for the rapid decrease in the strength of the correlations in the tropical North
549 Atlantic is due to relatively low correlations between JJA and ASO values of large-scale
550 parameters in that portion of the basin, indicating a lack of persistence in atmosphere/ocean
551 conditions when compared with the Caribbean (Table 4). The persistence of the 700 hPa RH and
552 850 hPa U fields in the tropical North Atlantic is especially low compared to other fields.

553 **3.4 Relationship between JJA DAOD and large-scale climate modes**

554 We next explore the relationship between JJA-averaged DAOD and two large-scale climate
555 modes that have been documented in many studies to impact Atlantic TC activity: ENSO (e.g.,
556 Gray, 1984; Goldenberg and Shapiro, 1996; Klotzbach, 2011; Klotzbach et al., 2018) and the
557 AMM (e.g., Kossin and Vimont, 2007; Patricola et al., 2014). El Niño typically reduces Atlantic
558 TC activity through several mechanisms including increasing westerly wind shear especially
559 over the Caribbean (Gray, 1984) and through upper-level tropospheric warming, causing
560 increased static stability and inhibiting deep convection (Tang and Neelin, 2004). The AMM has
561 also been suggested in prior research to significantly impact Atlantic TC activity (Kossin and
562 Vimont, 2007), especially when combined with ENSO (Patricola et al., 2014). A positive phase
563 of the AMM is associated with a warmer than normal tropical Atlantic, anomalously low sea
564 level pressure and anomalously weak trade winds - all of which favor Atlantic TC formation
565 (Kossin and Vimont, 2007).

566 Table 5 displays the correlations between JJA regionally-averaged DAODs from the different
567 aerosol reanalysis products and the JJA and ASO ENSO (as represented by the ONI) and AMM
568 indices. There is a positive correlation between JJA Caribbean DAOD and the concurrent
569 (significant at the 90% level) and ASO ONI (significant at the 95% level) using MRC and
570 NAAPS-RA, and the correlations with the ONI increase from JJA to ASO. The correlation
571 between JJA tropical North Atlantic DAOD and JJA/ASO ENSO is not significant, however,
572 consistent with previous studies (Lau and Kim, 2007; Doherty et al., 2014). ENSO events
573 climatologically intensify from boreal summer to boreal autumn (Harrison and Larkin, 1998),
574 which may be part of the reason for the increase in significance of the correlations from JJA to
575 ASO. In addition, this likely also explains part of the reason why Atlantic TC activity correlates

more strongly with Caribbean DAOD than with tropical Atlantic DAOD, given the pronounced impact that ENSO has on the Caribbean large-scale environment (Gray, 1984). Figure S3, in which JJA composites of MRC DAOD, 850 hPa horizontal wind and 700 hPa RH for the three top El Nino and La Nino ENSO years (based on JJA ONI) are shown, corroborates that stronger dust transport into Caribbean occurs during El Nino years without necessarily strong emissions over Africa and high DAOD over tropical North Atlantic. We also note that 2015 is both an El Niño and a high DAOD year, while 2011 is both a La Niña and low DAOD year. Removing the two overlapping years in the composites leads to similar results except that DAOD differences between El Nino and La Nino years are more negative in the tropical North Atlantic, additionally supporting the insignificant correlation between ENSO and tropical North Atlantic DAOD.

The correlations between JJA Caribbean DAOD and JJA AMM are consistently strong and negative (~-0.7) with all of the aerosol reanalyses (Table 5). As might be expected given that the signal of the AMM is climatologically strongest in the boreal spring and weakens in the boreal summer and fall (Kossin and Vimont, 2007), correlations of JJA DAOD are weaker with the ASO AMM than with the JJA AMM. Negative correlations are also obtained between the JJA tropical North Atlantic DAOD and the JJA AMM, while the correlation with the ASO AMM is weak and not statistically significant in general. The negative correlations between JJA DAODs and the AMM are consistent with Evan et al. (2011)'s study on the radiative effect of dust aerosols on the AMM. That study showed DAOD to be not only negatively correlated with the AMM but that its variability was found to excite the AMM on interannual to decadal time scales.

So far we have shown that Caribbean DAOD is correlated with Atlantic basin-wide ACE as well as two-large scale climate modes: ENSO and the AMM. Both of these modes have been shown to also impact Atlantic TC activity. To remove the influence of these climate indices from the relationship between DAOD and ACE, we use partial correlation analysis (Sharma et al., 1978). Table 6 shows the partial correlation matrix between JJA Caribbean and tropical North Atlantic DAOD and annual Atlantic basin-wide ACE while controlling for the ONI and AMM indices, respectively. Removing the influence of ENSO causes little change in the negative correlation between MRC Caribbean JJA DAOD and ACE. The correlation remains statistically significant, suggesting that ENSO is not primarily responsible for the negative correlation between Caribbean DAOD and Atlantic ACE, at least during the study period. The correlation between tropical North Atlantic JJA DAOD and ACE also changes little, although the correlation is weak and not statistically significant initially. We note that the correlation between ONI and ACE is very weak and is not significant during the 2003-2018 study period, partially due to the extremely active 2004 Atlantic hurricane season which occurred despite a weak El Niño event.

In contrast to the findings of removing ENSO from the DAOD-ACE relationship, after removing the influence of the AMM, the correlation between Caribbean JJA DAOD and Atlantic ACE is much weaker and drops to insignificant levels, suggesting that the AMM is an important factor in the dust-TC relationship. However, it is hard to argue that the AMM is the determining factor in the dust-TC relationship, as the correlation of ACE with JJA Caribbean DAOD is slightly higher than with the JJA AMM (-0.61 vs. 0.59). When the partial correlation is calculated between the AMM and ACE while removing the Caribbean dust (DAOD) influence, the correlation drops from 0.59 to an insignificant level ($r = \sim 0.26$), independent of season examined. This indicates that Caribbean DAOD is, in turn, an important factor in the AMM-TC relationship. When the TATL JJA DAOD is removed, the correlation between AMM and ACE is also reduced, implying

620   that the AMM/DAOD/TC relationship is strongly intertwined. This is physically feasible, as the
621   dust radiative forcing can result in cooler SST, which can introduce anomalously high sea level
622   pressure and stronger trade winds (and therefore stronger vertical wind shear), which is
623   characteristic of a negative AMM. This air-sea coupled response to dust radiative forcing can act
624   over relatively short timescales (e.g., one to two months) (Evan et al. 2011). Additionally, the
625   dryness of the dusty air and the radiative heating of the dust layer, can lead to stronger vertical
626   wind shear and a more stable lower atmosphere, all in line with a negative AMM that creates an
627   environment that is detrimental for TC formation and development. It could be argued that the
628   negative correlation between DAOD and Atlantic TC activity may be a result of forcing of the
629   AMM by African dust.

4. Sensitivity tests

631   The sensitivity of our results to the domain definitions of the tropical North Atlantic and the
632   Caribbean regions is explored by defining equal areas (shifting the separation longitude to
633   52.5°W) for the two regions within the MDR, as well as by expanding the two regions by 5°
634   latitude to the north (e.g., to 25°N). Neither of the two new definitions for regions significantly
635   change the correlations between JJA regionally averaged DAOD and large-scale fields (Table
636   S1, S2). The correlations between the JJA Caribbean DAOD and ACE are -0.59/-0.58 for the
637   longitudinal and latitudinal shift respectively, only slightly lower than -0.61 using the default
638   regional definitions. The correlations between the JJA TATL DAOD and ACE remain
639   insignificant (Table S3).

640   While airborne dust can impact TC activity, once TCs form and develop, both precipitation and
641   strong winds can significantly remove these dust particles. However, the removal effect by TCs
642   cannot primarily explain the negative DAOD-TC relationship. This is because peak dust activity
643   occurs from June to August with larger DAOD in June and July than in August over the Atlantic,
644   suggesting that peak DAOD in general leads the peak TC season by ~1-2 months (Figure S1).
645   Using June-July average DAOD instead of June-August average DAOD changes our results only
646   slightly. For example, the correlation between June-July Caribbean DAOD and Atlantic ACE is -
647   0.58, only slightly lower than that using JJA DAOD ($r = -0.61$) (Table S3). This has implications
648   for using DAOD as an indicator for seasonal TC forecasts which are often updated in early
649   August.

650   The sensitivity of the composite analysis of high versus low JJA Caribbean DAOD years to the
651   number of years is also explored by using two and four years for composites in addition to three
652   years (Table S4). Consistent results are found across all sensitivity tests. Atlantic basin-wide
653   numbers of tropical depressions, named storms, hurricanes and major hurricanes, and ACE are
654   higher (by a factor of 1.6-5) in the low than in the high JJA Caribbean DAOD seasons. The ratios
655   of observed average seasonal Atlantic hurricanes and major hurricanes in the low versus the high
656   JJA Caribbean DAOD seasons are generally higher than those of tropical depressions and named
657   storms, suggesting a stronger correlation relationship between dust aerosols and intense storms
658   than weak storms.

5. Conclusions and Discussions

660   The relationship between African dust and Atlantic tropical cyclone (TC) activity has been
661   analyzed in many prior studies (e.g., Dunion and Velden 2004; Evan et al. 2006a; Braun et al.

662 2013; Pan et al. 2018). This study has revisited this relationship with a statistical analysis using
663 three newly available aerosol reanalyses: the Naval Aerosol Analysis and Prediction System
664 reanalysis (NAAPS-RA), the Modern-Era Retrospective analysis for Research and Applications,
665 Version 2 (MERRA-2) aerosol reanalysis, the Copernicus Atmosphere Monitoring Service
666 ReAnalysis (CAMSRA), and a multi-reanalysis-consensus (MRC) based on the three reanalyses
667 for the period 2003-2018. The datasets are validated with ground-based observations for modal
668 (fine, coarse and total) aerosol optical depth (AOD). The MRC data is primarily used in this
669 study as it generally has better verification results than any of the individual reanalysis products.
670 To our knowledge, this is the first climate study using a multi-reanalysis consensus to represent
671 aerosol conditions. Our findings are summarized below:

672 1. Total AOD of the three aerosol reanalysis products are similar for the Atlantic Main
673 Development Region, however, AOD attributed to individual aerosol species (such as
674 dust aerosols) can be quite different among the three reanalysis products (Figure 4). June-
675 July-August (JJA) dust AOD (DAOD) magnitude can differ by as much as 0.06,
676 corresponding to approximately 60% of the climatological JJA DAOD based on MRC for
677 the Caribbean, and can differ by as much as 0.05, approximately 20% of the
678 climatological JJA DAOD based on MRC for the tropical North Atlantic. This is because
679 total AOD is the only aerosol property constrained by satellite observations through AOD
680 data assimilation in all three aerosol reanalysis products, while speciated AOD is not
681 constrained. This also supports the potential usefulness of MRC, as multi-model-
682 consensus are found to generally be better performers than individual models in aerosol
683 simulations (Sessions et al., 2015; Xian et al., 2019). Despite differences in DAOD
684 magnitude, DAODs of the three reanalysis products correlate significantly over the
685 tropical Atlantic and Caribbean.

686 2. Each of the three individual reanalyses and the MRC have significant and negative
687 correlations between JJA Caribbean DAOD and seasonal Atlantic Accumulated Cyclone
688 Energy (ACE) (Table 2). High JJA DAOD in the Caribbean is associated with a less
689 conducive environment for hurricane activity as represented by cooler SST, enhanced
690 vertical wind shear, lower mid-level moisture, and by lower Maximum Potential Intensity
691 (MPI) and Genesis Potential Index (GPI) values (Table 3). Pronounced differences in
692 Atlantic TC activity are seen when examining the three seasons with the highest levels of
693 JJA Caribbean DAOD compared with the three seasons with the lowest JJA Caribbean
694 DAOD (Table 4 and Figure 7). About three times as many major hurricanes occurred
695 during the three lowest DAOD seasons (2005, 2011, 2017) compared with the three
696 highest DAOD seasons (2018, 2015, 2014). Atlantic TC activity is also negatively
697 correlated with tropical North Atlantic DAOD but not as significantly as with Caribbean
698 DAOD for possible reasons discussed in the conclusion that follows.

699 3. High Caribbean DAOD is typically associated with El Niño conditions, however ENSO
700 does not appear to significantly impact the Caribbean DAOD-ACE relationship. The
701 robust DAOD-ACE correlation still holds after removing ENSO's influence via partial
702 correlation analysis.

703 4. JJA north Atlantic DAOD and the Atlantic Meridional Mode (AMM) are intertwined in
704 the dust-TC relationship. Both the Caribbean and tropical North Atlantic DAODs have
705 strong negative correlations with JJA values of the AMM index (with a stronger

706   correlation for the Caribbean DAOD). Meanwhile, the JJA AMM index correlates
707   significantly with Atlantic ACE. For AMM and DAOD, removing the other in their
708   relationships with ACE dramatically reduces the significance of the correlations based on
709   partial correlation analysis. This result supports Evan et al.(2011)'s work, which showed
710   that African dust excited AMM variability on interannual to decadal time scales through
711   radiative forcing of the underlying SST. Consequently, it can be argued that the negative
712   correlation between Caribbean and tropical North Atlantic DAOD and Atlantic TC
713   activity may be a result of forcing of the AMM by African dust.

714 These results agree with previous studies that showed negative correlations between boreal
715 summer Atlantic dustiness and TC activity (e.g., Dunion and Velden, 2004; Evan et al., 2006a;
716 Lau and Kim 2007). The correlations obtained in this study, especially those with Caribbean
717 DAOD, are slightly higher than previous studies, including correlations between boreal summer
718 dustiness and ACE (Evan et al., 2006a; Lau and Kim 2007) and between JJA dustiness and
719 ENSO (DeFlorio et al., 2016). We note that the study areas, time periods and study methods are
720 not identical between our study and these previous studies, implying the usefulness of aerosol
721 reanalyses in climate studies. Various sensitivity tests show that our results are not sensitive to
722 the definitions of areas for the Caribbean and tropical North Atlantic, the number of composite
723 years used, or the definition of the dust season (June-July vs. June-August).

724 Our results also document statistically significant relationships between Atlantic dustiness and
725 large-scale fields (e.g., SST, vertical wind shear, mid-level moisture and relatively vorticity) and
726 integrated TC diagnostic indices (e.g., MPI and GPI), which can be seen as confounding factors
727 in the dust-TC relationship. Exploring the causality of the documented negative correlation
728 between DAOD and Atlantic TC activity through modeling experiments is beyond the scope of
729 this paper. However in some modeling studies, radiative forcing of the scattering dust alone
730 could result in an inverse relationship between African dust and Atlantic TC activity (Dunstone
731 et. al, 2013; Strong et al., 2018; Sobel et al., 2019), along with consistent large-scale fields
732 associated with TC activity. So it is possible that radiative forcing of the scattering dust is a
733 dominant factor in the inverse dust-TC relationship on seasonal-interannual and basin-wide
734 scales. After all, aerosols are coupled radiatively with meteorology in the ERA-Interim dataset,
735 which provides the large-scale atmospheric data used in this study.

736 The correlations with Atlantic ACE are higher for Caribbean DAOD than for tropical North
737 Atlantic DAOD - a result that was not documented previously. The differences in the
738 relationships of Atlantic ACE with regional DAOD are potentially due to several factors:

739 a)   The large-scale environmental fields investigated herein are better self-correlated
740 between the JJA and ASO seasons over the Caribbean than over the tropical North Atlantic
741 (Table 4). Therefore, the higher correlation with JJA Caribbean DAOD, which reflects the large-
742 scale circulation, especially for the low- and mid-level wind flow that modulates how far African
743 dust can be transported, tends to extend into the ASO peak TC season. As was shown in
744 Saunders et al. (2017), the strength of the low-level winds in the Caribbean tends to be the most
745 robust diagnostic for seasonal ACE during the peak months of the Atlantic hurricane season.

746 b)   ENSO has a large impact on the Caribbean large-scale environment (Gray, 1984). ENSO-
747 forced SST anomalies typically exhibit very strong persistence from JJA to ASO (Harrison and

Larkin, 1998). As Caribbean JJA DAOD is correlated with ENSO to some extent, it is also correlated with Atlantic ACE.

c)   There might be a regime shift in the integrated outcome of dust-TC interactions from east to west across the tropical North Atlantic at climate time scales, with the eastern tropical North Atlantic (e.g., close to the African continent) having a positive correlation (e.g., since dust emission is often associated with AEWs emerging from Africa; Jones et al., 2003; Karyampudi and Carlson, 1988) while the correlation becomes more negative heading west across the basin.

d)   The relatively larger JJA DAOD variability in the Caribbean (larger relative dynamical range of Caribbean JJA DAOD compared to the tropical north Atlantic JJA DAOD over 2003-2018) could contribute to a higher correlation (Figures 3 and 4).

e)   AOD data quality is comparatively better over the Caribbean than over the tropical north Atlantic (Table 1; Figure 3), given that AOD reanalyses generally perform better over long-range transport regions than they do closer to the aerosol source regions (Xian et al., 2016).

The conclusions drawn from this study are based on 16-year records (2003-2018) of DAOD data from the MRC. We acknowledge that this analysis represents a relatively short timespan for a climate correlation study. Longer-period aerosol reanalyses with good fidelity are needed for further climate studies. These reanalyses face several challenges including dealing with changes to the network of AOD-observing satellites over time, as well as reasonable simulations and partitioning of aerosol-speciated AODs associated with rare severe aerosol events (e.g., volcanic eruptions) within AOD data assimilation systems.

It is also worth noting that the 2003-2018 DAOD climatology for the Atlantic MDR could be low relative to the extremely dusty period of the 1980s that has been documented by long-term in-situ dust concentration measurements made in Barbados (Prospero, 2014) and a 24-year eastern North Atlantic dust cover record derived from the Advanced Very High Resolution Radiometer (AVHRR, Evan et al., 2006). Dust concentration records at Barbados (1965-2011) and dust cover determined from AVHRR (1982-2005) both indicate that dust levels over the North Atlantic peaked during the mid-1980s, when tropical Atlantic TC activity was relatively low (e.g., Wang et al., 2012). Our findings are consistent with the negative correlations reflected in both the earlier dust and the earlier tropical Atlantic TC activity records.

Since we note that JJA/JJ Caribbean DAOD are strongly correlated with large-scale atmospheric fields which are frequently used in seasonal hurricane forecasts, DAOD may be a useful confirmation tool for observed thermodynamic conditions. Most groups issuing seasonal hurricane forecasts provide an update in early August (immediately prior to the peak of the Atlantic hurricane season). So early season (June-July) DAOD, especially over the Caribbean, could be a potential indicator for the strength of seasonal Atlantic TC activity. While there is very strong agreement between large-scale zonal wind fields (e.g., the June-July-averaged 850 hPa zonal wind over the tropical Atlantic correlates at 0.92 between ERA-Interim and MERRA-2, in which impact of aerosols on radiation and thereby on meteorology is included), there is less agreement with the mid-level moisture field. The correlation between ERA-Interim and MERRA-2 700 hPa RH over the tropical Atlantic averaged over June-July is only 0.72. The DAOD could potentially be used to help clarify the favorability/unfavorability of the

789 thermodynamic environment, as indicated also by the strong correlation between JJA Caribbean
790 DAOD and JJA and ASO MPI.

791 We believe this study, which shows a robust correlation relationship for the integrated dust-
792 atmosphere-ocean system, could provide a framework to better understand the linkages between
793 DAOD and Atlantic TC activity and how DAOD affects the large-scale environment of the
794 MDR. We find that DAOD in both the tropical Atlantic and Caribbean is negatively correlated
795 with Atlantic hurricane frequency, intensity and integrated indices such as ACE, with stronger
796 negative correlations in the Caribbean than farther east in the tropical North Atlantic. However,
797 this study focuses on seasonal to interannual time scales and provides analysis from a large-scale
798 point of view. Finer temporal scales (from hours to days) are needed in future studies for cases
799 where African dust is entrained into TC vortices.

800 **Acknowledgments:**
801 NAAPS-RA development and application and authors P. Xian and J.S. Reid are supported by the
802 Office of Naval Research Code 322. P. Klotzbach would like to acknowledge a grant from the G.
803 Unger Vetlesen Foundation. P. Colarco is supported by the NASA Modeling, Analysis, and
804 Prediction program (program manager: David Considine).

805
806 **Data Availability:** All data supporting the conclusions of this manuscript are available through
807 the links provided below:
808 AERONET Version 3 Level 2 data: http://aeronet.gsfc.nasa.gov
809 AMM index:
810 https://www.esrl.noaa.gov/psd/data/timeseries/monthly/AMM/ammsst.data
811 CAMSRA AOD: https://www.ecmwf.int/en/research/climate-reanalysis/cams-reanalysis
812 ENSO index:
813 http://origin.cpc.ncep.noaa.gov/products/analysis_monitoring/ensostuff/ONI_v5.php
814 ERA-interim monthly means: https://rda.ucar.edu/datasets/ds627.1/
815 HURDAT2:
816 https://www.aoml.noaa.gov/hrd/hurdat/hurdat2.html
817 MERRA-2 AOD:
818 https://disc.gsfc.nasa.gov/datasets/M2TMNXAER_V5.12.4/summary?keywords=%22MERRA-
819 2%22
820 NAAPS RA AOD: https://usgodae.org//cgi-
821 bin/datalist.pl?dset=nrl_naaps_reanalysis&summary=Go
822 NOAA OI SST V2 data: https://www.esrl.noaa.gov/psd/

823
824 **Author contribution:** P. J. K, J. P. D. and P.X. conceived the idea. P.X. and P.J.K performed
825 most of the analysis and writing. M.A.J. calculated and performed the analyses on MPI and GPI.
826 All authors contributed to the writing and revision of the manuscript.

827
828 **Competing interests:** The authors declare that they have no conflict of interest.

829

830 **References**
831 Barnston, A. G., Chelliah, M., and Goldenberg, S. B.: Documentation of a highly ENSO-related
832 SST region in the equatorial Pacific. Atmosphere-Ocean, 35(3), 367-383.
833 https://doi.org/10.1080/07055900.1997.9649597, 1997.

834 Bell, G. D., Halpert, M. S., Schnell, R. C., Higgins, R. W., Lawrimore, J., Kousky, V. E., et al. :
835 Climate assessment for 1999. Bulletin of the American Meteorological Society, 81(6), S1-S50.
836 https://doi.org/10.1175/1520-0477(2000)81[s1:CAF]2.0.CO;2, 2000.
837 Bercos-Hickey, E., Nathan, T. R., and Chen, S. H. : Saharan dust and the African easterly jet-
838 African easterly wave system: Structure, location and energetics. Quarterly Journal of the Royal
839 Meteorological Society, 143(708), 2797-2808. https://doi.org/10.1002/qj.3128, 2017.
840 Bister, M., and Emanuel, K. A.: Low frequency variability of tropical cyclone potential intensity.
841 1. Interannual to interdecadal variability. J. Geophys. Res., 107, 4801,
842 doi:10.1029/2001JD000776., 2002.
843 Braun, S. A., Sippel, J. A., Shie, C.-L., and Boller, R. A. : The evolution and role of the Saharan
844 air layer during Hurricane Helene (2006). Monthly Weather Review, 141(12), 4269–4295.
845 https://doi.org/10.1175/MWR-D-13-00045.1, 2013.
846 Braun, S. A. : Re-evaluating the role of the Saharan Air Layer in Atlantic tropical cyclogenesis
847 and evolution. Monthly Weather Review, 138(6), 2007–2037.
848 https://doi.org/10.1175/2009MWR3135.1, 2010.
849 Bretl, S., Reutter, P, Raible, C. C., Ferrachat, S., Poberaj, C. S., Revell, L. E., and Lohmann, U.:
850 The influence of absorbed solar radiation by Saharan dust on hurricane genesis. Journal of
851 Geophysical Research: Atmospheres, 120(5), 1902–1917.
852 https://doi.org/10.1002/2014JD022441, 2015.
853 Buchard, V., Randles. C. A., da Silva, A., Darmenov, A. S., Colarco, P. R., Govindaraju, R.C., et
854 al.: The MERRA-2 Aerosol Reanalysis, 1980-onward, Part II: Evaluation and case studies.
855 Journal of Climate, 30(17), 6851-6872. https://doi.org/10.1175/JCLI-D-16-0613.1, 2017.
856 Carlson, T. N., and Prospero, J. M. : The large-scale movement of Saharan air outbreaks over the
857 northern equatorial Atlantic. Journal of Applied Meteorology, 11(2), 283–297.
858 https://doi.org/10.1175/1520-0450(1972)011<0283:TLSMOS>2.0.CO;2, 1972.
859 Camargo, S. J., Emanuel, K. A. and Sobel, A. H. : Use of a genesis potential index to diagnose
860 ENSO effects on tropical cyclone genesis. J. Clim. 20, 4819–4834, 2007.
861 Chin, M., Rood, R., Lin, S., Muller J., and Thompson, A.: Atmospheric sulfur cycle simulated in
862 the global model GOCART: Model description and global properties. Journal of Geophysical
863 Research: Atmospheres, 105(D20), 24,671–24,687. https://doi.org/10.1029/2000JD900384,
864 2000.
865 Colarco, P. R., Toon, O. B., Reid, J. S., Livingston, J. M., Russell, P. B., Redemann, J., et
866 al.:Saharan dust transport to the Caribbean during PRIDE: 2. Transport, vertical profiles, and
867 deposition in simulations of in situ and remote sensing observations. Journal of Geophysical
868 Research: Atmospheres, 108(D19), 8590, https://doi.org/10.1029/2002JD002659, 2003.
869 Colarco, P., da Silva, A., Chin, M., and Diehl, T.: Online simulations of global aerosol
870 distributions in the NASA GEOS-4 model and comparisons to satellite and ground-based aerosol
871 optical depth, Journal of Geophysical Research: Atmospheres, 115(D14207),
872 https://doi.org/10.1029/2009JD012820, 2010.
873 Dee, D. P., Uppala, S. M., Simmons, A. J., Berrisford, P., Poli, P., Kobayashi, S., Andrae, U., et
874 al.: The ERA-Interim reanalysis: configuration and performance of the data assimilation system.
875 Quarterly Journal of the Royal Meteorological Society, 137(656), 553-597.
876 https://doi.org/10.1002/qj.828, 2011.
877 DeFlorio, M. J., Goodwin, I. D., Cayan, D. R., Miller, A. J., Ghan, S. J., Pierce, D. W., Russell,
878 L. M., et al.: Interannual modulation of subtropical Atlantic boreal summer dust variability by
879 ENSO. Climate Dynamics, 46(1), 585-599. https://doi.org/10.1007/s00382-015-2600-7, 2016.

880 DeMott, P., Sassen, K., Poellot, M., Baumgardner, D., Rogers, D., Brooks, S. D., Prenni, A. J.,
881 and Kreidenweis, S. M.: African dust aerosols as atmospheric ice nuclei. Geophysical Research
882 Letters, 30, 1732. https://doi.org/10.1029/2003GL017410, 2003.
883 Doherty, O. M., Riemer, N., and Hameed, S.: Saharan mineral dust transport into the Caribbean:
884 Observed atmospheric controls and trends, Journal of Geophysical Research: Atmospheres,
885 113(D07211). https://doi.org/10.1029/2007JD009171, 2008.
886 Dunion, J. P.: Re-writing the climatology of the tropical North Atlantic and Caribbean Sea
887 atmosphere. Journal of Climate, 24(3), 893–908. https://doi.org/10.1175/2010JCLI3496.1, 2011.
888 Dunion, J. P., andand Marron, C. S. : A reexamination of the Jordan mean tropical sounding
889 based on awareness of the Saharan air layer: Results from 2002. Journal of Climate, 21(20),
890 5242–5253. https://doi.org/10.1175/2008JCLI1868.1, 2008.
891 Dunion, J. P., and Velden, C. S. : The impact of the Saharan Air Layer on Atlantic tropical
892 cyclone activity. Bulletin of the American Meteorological Society, 85(3), 353-365.
893 https://doi.org/10.1175/BAMS-85-3-353, 2004.
894 Emanuel, K. A., and Nolan, D. S. :2004 Tropical cyclone activity and global climate. In: Proc. of
895 26th Conference on Hurricanes and Tropical Meteorology, pp. 240–241, American
896 Meteorological Society , Miami, FL., 2004.
897 Engelstaedter, S., and Washington, R.: Atmospheric controls on the annual cycle of North
898 African dust, Journal of Geophysical Research: Atmospheres, 112(D3), D03103.
899 https://doi.org/10.1029/2006JD007195, 2007.
900 Evan, A.T., Dunion, J. P., Foley, J. A., Heidinger, A. K., and Velden, C. S. : New evidence for a
901 relationship between Atlantic tropical cyclone activity and African dust outbreaks. Geophysical
902 Research Letters, 33, L19813. https://doi.org/10.1029/2006GL026408, 2006a.
903 Evan, A. T., Heidinger, A. K., and Knippertz P.: Analysis of winter dust activity off the coast of
904 West Africa using a new 24-year over-water advanced very high resolution radiometer satellite
905 dust climatology. Journal of Geophysical Research: Atmospheres, 111(D12), D12210.
906 https://doi.org/10.1029/2005JD006336, 2006b.
907 Evan, A. T., Foltz, G. R., Zhang, D., and Vimont D. J. : Influence of African dust on ocean–
908 atmosphere variability in the tropical Atlantic. Nature Geoscience.4, 762–765.
909 https://doi.org/10.1038/ngeo1276, 2011.
910 Evan, A. T., Vimont, D. J., Heidinger, A. K., Kossin, J. P., and Bennartz, R.: The role of aerosols
911 in the evolution of tropical North Atlantic Ocean temperature anomalies. *Science,* 324(5928),
912 778-781. https://doi.org/10.1126/science.1167404, 2009.
913 Flemming, J., Benedetti, A., Inness, A., Engelen, R. J., Jones, L., Huijnen, V., Remy, S.,
914 Parrington, M., Suttie, M., Bozzo, A., Peuch, V.-H., Akritidis, D., and Katragkou, E.: The
915 CAMS interim Reanalysis of Carbon Monoxide, Ozone and Aerosol for 2003–2015, Atmos.
916 Chem. Phys., 17, 1945–1983, https://doi.org/10.5194/acp-17-1945-2017, 2017.
917 Giles, D. M., Sinyuk, A., Sorokin, M. G., Schafer, J. S., Smirnov, A., Slutsker, I., Eck, T. F., et
918 al.: Advancements in the Aerosol Robotic Network (AERONET) Version 3 database –
919 automated near-real-time quality control algorithm with improved cloud screening for Sun
920 photometer aerosol optical depth (AOD) measurements. Atmospheric Measurement Techniques,
921 12(1), 169-209, https://doi.org/10.5194/amt-12-169-2019, 2019.
922 Goldenberg, S. B., Landsea, C. W., Mestas-Nuñez, A. M., and Gray, W. M.: The recent increase
923 in Atlantic hurricane activity: Causes and implications. Science, 293(5529), 474-479.
924 https://doi.org/10.1126/science.1060040, 2001.

Goldenberg, S. B., and Shapiro, L. J.: Physical mechanisms for the association of El Niño and West African rainfall with Atlantic major hurricane activity. Journal of Climate, 9(6), 1169-1187. https://doi.org/10.1175/1520-0442(1996)009%3C1169:PMFTAO%3E2.0.CO;2, 1996.

Gray, W. M.: Global view of the origin of tropical disturbances and storms. Monthly Weather Review, 96(10), 669-700. https://doi.org/10.1175/1520-0493(1968)096%3C0669:GVOTOO%3E2.0.CO;2, 1968,

Gray, W. M.: Atlantic seasonal hurricane frequency. Part I: El Niño and 30 mb quasi-biennial oscillation influences. Monthly Weather Review, 112(9), 1649-1668. https://doi.org/10.1175/1520-0493(1984)112%3C1649:ASHFPI%3E2.0.CO;2, 1984.

Grogan, D. F. P., Nathan, T. R., Chen, S. H.: Effects of Saharan dust on the linear dynamics of African easterly waves. Journal of Atmospheric Science, 73(2), 891–911. https://doi.org/10.1175/JAS-D-15-0143.1, 2016.

Grogan, D. F. P., Nathan, T. R., Chen, S. H.: Saharan dust and the nonlinear evolution of the African easterly jet–African easterly wave system. Journal of Atmospheric Science, 74(1), 27–47. https://doi.org/10.1175/JAS-D-16-0118.1, 2017.

Harrison, D. E., Larkin, N. K.: El Niño-Southern Oscillation sea surface temperature and wind anomalies, 1946-1993. Reviews of Geophysics, 36(3), 353-400. https://doi.org/10.1029/98RG00715, 1998.

Herbener, S. R., van den Heever, S. C., Carrio, G. G., Saleeby, S. M., Cotton W. R.: Aerosol indirect effect on idealized tropical cyclone dynamics. Journal of Atmospheric Science, 71, 2040-2055. https://doi.org/10.1175/JAS-D-13-0202.1, 2014.

Herbener, S. R., Saleeby, S. M., van den Heever, S. C., and Twohy, C. H.: Tropical storm redistribution of Saharan dust to the upper troposphere and ocean surface, Geophys. Res. Lett., 43, doi:10.1002/2016GL070262, 2016.

Holben, B. N., Eck, T. F., Slutsker, I, Tanre, D., Buis, J. P., Setzer, A., et al.: AERONET - A federated instrument network and data archive for aerosol characterization, Remote Sensing of the Environment, 66(1), 1-16. https://doi.org/10.1016/S0034-4257(98)00031-5, 1998.

Holben, B. N., Tanré, D., Smirnov, A., Eck, T. F., Slutsker, I, Abuhassan, N., et al.: An emerging ground-based aerosol climatology: Aerosol optical depth from AERONET, Journal of Geophysical Research: Atmospheres, 106(D11), 12067-12097. https://doi.org/10.1029/2001JD900014, 2001.

Holland, G. J.: The maximum potential intensity of tropical cyclones. J. Atmos. Sci., **54**, 2519–2541, https://doi.org/10.1175/1520-0469(1997)054<2519:TMPIOT>2.0.CO;2, 1997.

Hsu, N. C., Gautam, R., Sayer, A. M., Bettenhausen, C., Li, C., Jeong, M. J., et al.: Global and regional trends of aerosol optical depth over land and ocean using SeaWiFS measurements from 1997 to 2010. Atmospheric Chemistry and Physics, 12, 8037-8053. https://doi.org/10.5194/acp-12-8037-2012, 2012.

Hyer, E. J., Reid, J. S., and Zhang, J.: An over-land aerosol optical depth data set for data assimilation by filtering, correction, and aggregation of MODIS Collection 5 optical depth retrievals. Atmospheric Measurement Techniques, 4(3), 379-408. https://doi.org/10.5194/amt-4-379-2011, 2011.

Inness, A., Baier, F., Benedetti, A., Bouarar, I., Chabrillat, S., Clark, H., Clerbaux, C., Coheur, P., Engelen, R. J., Errera, Q., Flemming, J., George, M., Granier, C., Hadji-Lazaro, J., Huijnen, V., Hurtmans, D., Jones, L., Kaiser, J. W., Kapsomenakis, J., Lefever, K., Leitão, J., Razinger, M., Richter, A., Schultz, M. G., Simmons, A. J., Suttie, M., Stein, O., Thépaut, J.-N., Thouret, V., Vrekoussis, M., Zerefos, C., and the MACC team: The MACC reanalysis: an 8 yr data set of

atmospheric composition, Atmos. Chem. Phys., 13, 4073–4109, https://doi.org/10.5194/acp-13-4073-2013, 2013.

Inness, A., Ades, M., Agustí-Panareda, A., Barré, J., Benedictow, A., Blechschmidt, A.-M., Dominguez, J. J., Engelen, R., Eskes, H., Flemming, J., Huijnen, V., Jones, L., Kipling, Z., Massart, S., Parrington, M., Peuch, V.-H., Razinger, M., Remy, S., Schulz, M., and Suttie, M.: The CAMS reanalysis of atmospheric composition, Atmos. Chem. Phys., 19, 3515–3556, https://doi.org/10.5194/acp-19-3515-2019, 2019.

Jenkins, G. S., Pratt, A. S. and Heymsfield, A.: Possible linkages between Saharan dust and tropical cyclone rain band invigoration in the eastern Atlantic during NAMMA-06. Geophysical Research Letters, 35, L08815. https://doi.org/10.1029/2008GL034072, 2008.

Jones, T. A., Cecil, D. J. and Dunion, J.: The environmental and inner-core conditions governing the intensity of Hurricane Erin (2001). Weather and Forecasting, 22(4), 708–725. https://doi.org/10.1175/WAF1017.1, 2007.

Jones, C., Mahowald, N. M., and Luo, C. : The role of easterly waves on African desert dust transport. Journal of Climate, 16, 3617-3628, 2003

Jones, C., Mahowald, N. M., and Luo, C.: Observational evidence of African desert dust intensification of easterly waves. *Geophysical Research Letters*, 31(17), L17208. https://doi.org/10.1029/2004GL020107, 2004.

Joyce, R. J., Janowiak, J. E., Arkin, P. A., Xie, P. : CMORPH: A method that produces global precipitation estimates from passive microwave and infrared data at high spatial and temporal resolution. Journal of Hydrometeorology, 5(3), 487-503, https://doi.org/10.1175/1525-7541(2004)005%3C0487:CAMTPG%3E2.0.CO;2, 2004.

Kahn, R. A., and Gaitley, B. J.: An analysis of global aerosol type as retrieved by MISR. Journal of Geophysical Research: Atmospheres, 120(9), 4248–4281. https://doi.org/10.1002/2015JD023322, 2015.

Kaku, K. C., Reid, J. S., O'Neill, N. T., Quinn, P. K., Coffman, D. J., and Eck, T. F.: Verification and application of the extended spectral deconvolution algorithm (SDA+) methodology to estimate aerosol fine and coarse mode extinction coefficients in the marine boundary layer. Atmospheric Measurement Techniques, 7(10), 3399-3412. https://doi.org/10.5194/amt-7-3399-2014, 2014.

Karyampudi, V. M., and Carlson, T. N.: Analysis and numerical simulations of the Saharan air layer and its effect on easterly wave disturbances. Journal of the Atmospheric Sciences, 45(21), 3102–3136. https://doi.org/10.1175/1520-0469(1988)045<3102:AANSOT>2.0.CO;2, 1988.

Karyampudi, V. M., and Pierce, H. F.: Synoptic-scale influence of the Saharan Air Layer on tropical cyclogenesis over the eastern Atlantic. Monthly Weather Review, 130, 3100-3128, 2002.

Karydis, V. A., Kumar, P., Barahona, D., Sokolik, I. N. and Nenes, A.: On the effect of dust particles on global cloud condensation nuclei and cloud droplet number. Journal of Geophysical Research: Atmospheres, 116(D23204). https://doi.org/10.1029/2011JD016283, 2011.

Khain, A. P., Leung, L. R., Lynn, B., and Ghan, S.: Effects of aerosols on the dynamics and microphysics of squall lines simulated by spectral bin and bulk parameterization schemes. Journal of Geophysical Research: Atmospheres, 114(D22203). https://doi.org/10.1029/2009JD011902, 2009.

Klotzbach, P. J.: El Niño – Southern Oscillation's impact on Atlantic basin hurricanes and U.S. landfalls. Journal of Climate, 24(4), 1252-1263. https://doi.org/10.1175/2010JCLI3799.1, 2011.

Klotzbach, P. J., Bowen, S. G., Pielke Jr., R., Bell, M. M. : Continental United States landfall frequency and associated damage. Observations and future risks. Bulletin of the American Meteorological Society, 99(7), 1359-1376. https://doi.org/10.1175/BAMS-D-17-0184.1, 2018.

Knippertz, P., Todd, M. C.: The central west Saharan dust hot spot and its relation to African easterly waves and extratropical disturbances. Journal of Geophysical Research: Atmospheres, 115(D12117). https://doi.org/10.1029/2009JD012819, 2010.

Kossin, J. P., and Vimont, D. J.: A more general framework for understanding Atlantic hurricane variability and trends. Bulletin of the American Meteorological Society, 88(11), 1767–1782. https://doi.org/10.1175/BAMS-88-11-1767, 2007.

Kuciauskas, A. P., Xian, P., Hyer, E. J., Oyola, M. I. and Campbell, J. R. : Supporting weather forecasters in predicting and monitoring Saharan Air Layer dust events as they impact the Greater Caribbean. Bulletin of the American Meteorological Society, 99(2), 259-268. https://doi.org/10.1175/BAMS-D-16-0212.1, 2018.

Landsea, C. W. : A climatology of intense (or major) Atlantic hurricanes. Monthly Weather Review, 121(6), 1703-1713. https://doi.org/10.1175/1520-0493(1993)121%3C1703:ACOIMA%3E2.0.CO;2, 1993.

Landsea, C. W., and Franklin, J. L. : Atlantic hurricane database uncertainty and presentation of a new database format. Monthly Weather Review, 141(10), 3576-3592. https://doi.org/10.1175/MWR-D-12-00254.1, 2013.

Lau, W. K. M., and Kim, K.: How nature foiled the 2006 hurricane forecasts. Eos Transactions American Geophysical Union, 88(9), 105-107. https://doi.org/10.1029/2007EO090002, 2007.

Levy, R. C., et al. : Evaluation of the MODIS aerosol retrievals over ocean and land during CLAMS, J. Atmos. Sci., 62(4), 974–992, 2005.

Levy, R. C., Remer, L. A., Kleidman, R. G., Mattoo, S., Ichoku, C., Kahn, R., and Eck, T. F.: Global evaluation of the Collection 5 MODIS dark-target aerosol products over land. Atmospheric Chemistry and Physics, 10(21), 10399-10420. https://doi.org/10.5194/acp-10-10399-2010, 2010.

Lynch, P., Reid, J. S., Westphal, D. L., Zhang, J., Hogan, T. F., Hyer, E. A., et al.: An 11-year global gridded aerosol optical thickness reanalysis (v1.0) for atmospheric and climate sciences. Geoscientific Model Development, 9(4), 1489-1522. https://doi.org/10.5194/gmd-9-1489-2016, 2016.

Ma, P. L., Zhang, K., Shi, J. J., Matsui, T., and Arking, A.: Direct radiative effect of mineral dust on the development of African easterly waves in late summer, 2003–07. Journal of Applied Meteorology and Climatology, 51(12), 2090–2104. https://doi.org/10.1175/JAMC-D-11-0215.1, 2012.

Miller, R. L., and Tegen, I. : Climate response to soil dust aerosols. Journal of Climate, 11(12), 3247–3267. https://doi.org/10.1175/1520-0442(1998)011<3247:CRTSDA>2.0.CO;2, 1998.

Nathan, T. R., Grogan, D. F. P, and Chen, S. H.: Subcritical destabilization of African easterly waves by Saharan mineral dust. Journal of the Atmospheric Sciences, 74(4), 1039–1055. https://doi.org/10.1175/JAS-D-16-0247.1, 2017.

Nowottnick, E. P., Colarco, P. R., Braun, S. A., Barahona, D. O., da Silva, A., Hlavka, D. L., et al.: Dust impacts on the 2012 Hurricane Nadine track during the NASA HS3 field campaign. Journal of the Atmospheric Sciences, 75(7), 2473-2489. https://doi.org/10.1175/JAS-D-17-0237.1, 2018.

Nowottnick, E., Colarco, P., da Silva, A., Hlavka, D., and McGill, M.: The fate of Saharan dust across the Atlantic and implications for a central American dust barrier. Atmospheric Chemistry and Physics, 11(16), 8415-8431. https://doi.org/10.5194/acp-11-8415-2011, 2011.

O'Neill, N. T., Eck, T. F., Smirnov, A., Holben, B. N., and Thulasiraman, S. : Spectral discrimination of coarse and fine mode optical depth. Journal of Geophysical Research: Atmospheres, 108(D17), 4559. https://doi.org/10.1029/2002JD002975, 2003.

Pan, B., Wang, Y., Hu, J., Lin, Y., Hsieh, J-S, Logan, T. et al.,: Impacts of Saharan dust on Atlantic regional climate and implications for tropical cyclones. Journal of Climate, 31(18), 7621-744. https://doi.org/10.1175/JCLI-D-16-0776.1, 2018.

Patricola, C. M., Saravanan, R., and Chang, P. : The impact of the El Niño-Southern Oscillation and Atlantic Meridional Mode on seasonal Atlantic tropical cyclone activity. Journal of Climate, 27(14), 5311-5328. https://doi.org/10.1175/JCLI-D-13-00687.1, 2014.

Pratt, A. S., and Evans, J. L. : Potential impacts of the Saharan Air Layer on numerical model forecasts of North Atlantic tropical cyclogenesis. Weather and Forecasting, 24(2), 420-435. https://doi.org/10.1175/2008WAF2007090.1, 2008.

Prospero, J. M.: Long-term measurements of the transport of African mineral dust to the southeastern United States: Implications for regional air quality. Journal of Geophysical Research: Atmospheres, 104(D13), 15917–15927. https://doi.org/10.1029/1999JD900072, 1999.

Prospero, J. M. : Characterizing the temporal and spatial variability of African dust over the Atlantic. Past Global Changes Magazine, 22(2), 68-69. https://doi.org/10.22498/pages.22.2.68, 2014.

Prospero, J. M., and Lamb, P. J. : African droughts and dust transport to the Caribbean: Climate change implications. Science, 302(5647), 1024-1027. https://doi.org/10.1126/science.1089915, 2003.

Prospero, J. M., and Nees, R. T. : Impact of the North African drought and El Niño on mineral dust in the Barbados trade winds. Nature, 320, 735. https://doi.org/10.1038/320735a0, 1986.

Randles, C. A., daSilva, A. M., Buchard, V., Colarco, P. R., Darmenov, A., Govindaraju, R., et al.: The MERRA-2 aerosol reanalysis, 1980 onward. Part I: System description and data assimilation evaluation. Journal of Climate, 30(17), 6823-6850. https://doi.org/10.1175/JCLI-D-16-0609.1, 2017.

Reale, O., Lau, W. K., Kim, K. M., and Brin, E.: Atlantic tropical cyclogenetic processes during SOP-3 NAMMA in the GEOS-5 global data assimilation and forecast system. Journal of Atmospheric Sciences, 66(12), 3563–3578. https://doi.org/10.1175/2009JAS3123.1, 2009.

Reale, O., Lau, K. M, and da Silva, A. : Impact of interactive aerosol on the African easterly jet in the NASA GEOS-5 global forecasting system. Weather and Forecasting, 26(4), 504–519. https://doi.org/10.1175/WAF-D-10-05025.1, 2011.

Reed, K. A., Bacmeister, J. T., Huff, J. J. A., Wu, X., Bates, S. C., and Rosenbloom, N. A.: Exploring the impact of dust on North Atlantic hurricanes in a high-resolution climate model.Geophysical Research Letters, 46, 1105–1112. https://doi.org/10.1029/2018GL080642, 2019.

Reid, J. S., Kinney, J. E., Westphal, D. L., Holben, B. N., Welton, E. J., Tsay, S-C., et al.: Analysis of measurements of Saharan dust by airborne and ground-based remote sensing methods during the Puerto Rico Dust Experiment (PRIDE). Journal of Geophysical Research: Atmospheres, 108, 8586. https://doi.org/10.1029/2002JD002493, 2003.

Reynolds, R.W., Rayner, N. A., Smith, T. M., Stokes, D. C., and Wang, W.: An improved in situ and satellite SST analysis for climate. Journal of Climate, 15(13), 1609–1625. https://doi.org/10.1175/1520-0442(2002)015<1609:AIISAS>2.0.CO;2, 2002.

Riemer, N., Doherty, O. M., and Hameed, S. : On the variability of African dust transport across the Atlantic, Geophys. Res. Lett., 33, L13814, doi:10.1029/2006GL026163., 2006.

Rienecker, M. M., Suarez, M. J., Gelaro, R., Todling, R., Bacmeister, J., Liu, E., et al.: MERRA: NASA's Modern Era Retrospective Analysis for Research and Applications. Journal of Climate, 24(14), 3624-3648. https://doi.org/10.1175/JCLI-D-11-00015.1, 2011.

Rosenfeld, D., Khain, A., Lynn, B., and Woodley, W. L.: Simulation of hurricane response to suppression of warm rain by sub-micron aerosols. Atmospheric Chemistry and Physics, 7(13), 3411-3424. https://doi.org/10.5194/acp-7-3411-2007, 2007.

Sassen, K., DeMott, P. J., Prospero, J. M. and Poellot, M. R.: Saharan dust storms and indirect aerosol effects on clouds: CRYSTAL-FACE results. Geophysical Research Letters, 30(12), 1633. https://doi.org/10.1029/2003GL017371, 2003.

Saunders, M. A., Klotzbach, P. J., and Lea, A. S.: Replicating annual North Atlantic hurricane activity 1878-2012 from environmental variables. Journal of Geophysical Research: Atmospheres, 122(12), 6284-6297. https://doi.org/10.1002/2017JD026492, 2017.

Saunders, M. A., Klotzbach. P. J., Lea, A. S. R., Schreck, C. J., and Bell, M. M.: Quantifying the probability and causes of the surprisingly active 2018 North Atlantic hurricane season. Earth and Space Science, 7(3), 1-14, https://doi.org/10.1029/2019EA000852, 2020.

Sessions, W. R., Reid, J. S., Benedetti, A., Colarco, P. R., da Silva, A., Lu, S., Sekiyama, T., Tanaka, T. Y., Baldasano, J. M., Basart, S., Brooks, M. E., Eck, T. F., Iredell, M., Hansen, J. A., Jorba, O. C., Juang, H.-M. H., Lynch, P., Morcrette, J.-J., Moorthi, S., Mulcahy, J., Pradhan, Y., Razinger, M., Sampson, C. B., Wang, J., and Westphal, D. L.: Development towards a global operational aerosol consensus: basic climatological characteristics of the International Cooperative for Aerosol Prediction Multi-Model Ensemble (ICAP-MME), Atmos. Chem. Phys., 15, 335-362, 2015.

Sharma, S.S., Kleinbaum, D.G., and Kupper, L.L.: Applied Regression Analysis and Other Multivariate Methods. https://doi.org/10.2307/3150614, 1978.

Shi, Y., Zhang, J., Reid, J. S., Holben, B., Hyer, E. J., and Curtis, C.: An analysis of the collection 5 MODIS over-ocean aerosol optical depth product for its implication in aerosol assimilation, Atmospheric Chemistry and Physics, 11(2), 557-565. https://doi.org/10.5194/acp-11-557-2011, 2011.

Sippel, J. A., Braun, S. A., and Shie, C.-L.: Environmental influences on the strength of Tropical Storm Debby (2006). Journal of the Atmospheric Sciences, 68(11), 2557–2581. https://doi.org/10.1175/2011JAS3648.1, 2011.

Strong, J. D. O., Vecchi, G. A., andGinoux, P.: The climatological effect of Saharan dust on global tropical cyclones in a fully coupled GCM. Journal of Geophysical Research:Atmospheres, 123, 5538–5559.https://doi.org/10.1029/2017JD027808, 2018.

Sobel, A. H., Camargo, S. J. and Previdi, M.: Aerosol vs. greenhouse gas effects on tropical cyclone potential intensity and the hydrologic cycle. Journal of Climate, doi:10.1175/JCLI-D-18-0357.1, 2019.

Sun, D., Lau, K. M., and Kafatos, M.: Contrasting the 2007 and 2005 hurricane seasons: Evidence of possible impacts of Saharan dry air and dust on tropical cyclone activity in the Atlantic basin. Geophysical Research Letters, 35, L15405. https://doi.org/10.1029/2008GL034529, 2008.

Tang, B.H., and Neelin, J. D.: ENSO influence on Atlantic hurricanes via tropospheric warming. Geophysical Research Letters, 31(24), L24204. https://doi.org/10.1029/2004GL021072, 2004.

Tompkins A. M., Cardinali, C., Morcrette, J. J., and Rodwell, M.: Influence of aerosol climatology on forecasts of the African easterly jet. Geophysical Research Letters, 32(10), L10801. https://doi.org/10.1029/2004GL022189, 2005.

Tsamalis, C., Chedin, A., Pelon, J., and Capelle, V.: The seasonal vertical distribution of the Saharan Air Layer and its modulation by the wind. Atmospheric Chemistry and Physics, 13(22), 11235-11257. https://doi.org/10.5194/acp-13-11235-2013, 2013.

Towhy, C. H., Kreidenweis, S. M., Eidhammer, T., Browell, E.V., Heymsfield A. J., Bansemer, A. R., et al.: Saharan dust particles nucleate droplets in eastern Atlantic clouds. Geophysical Research Letters, 36, L01807. https://doi.org/10.1029/2008GL035846, 2009.

Wang, C., Dong, S., Evan, A. T., Foltz, G. R., and Lee, S.: Multidecadal covariability of North Atlantic sea surface temperature, African dust, Sahel rainfall and Atlantic hurricanes. Journal of Climate, 25(15), 5404-5415. https://doi.org/10.1175/JCLI-D-11-00413.1, 2012.

Westphal, D. L., Toon, O. B., and Carlson, T. N.: A two-dimensional numerical investigation of the dynamics and microphysics of Saharan dust storms, Journal of Geophysical Research: Atmospheres, 92, 3027 – 3049. https://doi.org/10.1029/JD092iD03p03027, 1987.

Wilcox, E. M., Lau, K. M., and Kim, K. M.: A northward shift of the North Atlantic Ocean intertropical convergence zone in response to summertime Saharan dust outbreaks. Geophysical Research Letters, 37(4), L04804. https://doi.org/10.1029/2009GL041774, 2010.

Xian, P., Reid, J. S., Turk, J. F., Hyer, E. J., and Westphal, D. L.: Impact of modeled versus satellite measured tropical precipitation on regional smoke optical thickness in an aerosol transport model. Geophysical Research Letters, 36, L16805. https://doi.org/10.1029/2009GL038823, 2009.

Xian, P., Reid, J. S., Hyer, E. J., Sampson, C. R., Rubin, J. I., Ades, M., et. al.: Current State of the global operational aerosol multi-model ensemble: an update from the International Cooperative for Aerosol Prediction (ICAP). Quarterly Journal of the Royal Meteorological Society. Published online Feb 4, 2019. https://doi.org/10.1002/qj.3497, 2019.

Zhang, H., McFarquhar, G. M., Cotton, W. R., and Deng, Y.: Direct and indirect impacts of Saharan dust acting as cloud condensation nuclei on tropical cyclone eyewall development. Geophysical Research Letters, 36, L06802. https://doi.org/10.1029/2009GL037276, 2009.

Zhang, H., McFarquhar, G. M., Saleeby, S. M., and Cotton, W. R.: Impacts of Saharan dust as CCN on the evolution of an idealized tropical cyclone. Geophysical Research Letters, 34, L14812. https://doi.org/10.1029/2007GL029876, 2007.

Zhang, J., and Reid, J. S. : MODIS aerosol product analysis for data assimilation: Assessment of over-ocean level 2 aerosol optical thickness retrievals. Journal of Geophysical Research: Atmospheres, 111(D22207). https://doi.org/10.1029/2005JD006898, 2006.

Zhang, J., Reid, J. S., R. Alfaro-Contreras, R. and Xian, P: : Has China been exporting less particulate air pollution over the past decade?, Geophys. Res. Lett., 44, 2941–2948, doi:10.1002/2017GL072617, 2017.

Tables:

Table 1. Root mean square error of total AOD (left number in each cell) and coarse-mode AOD (right number in each cell) at 550nm from individual aerosol reanalyses, including CAMSRA, MERRA-2, NAAPS-RA, and the Multi-Reanalysis-Consensus (MRC) verified with AERONET V3L2 monthly data for the 2003-2018 time period. The rank of MRC among all reanalyses in terms of RMSE is also shown. "~" means there are ties in the ranking. The first five sites are located in North Africa or off of the northwestern coast of Africa. The last four sites are located in or near the Caribbean Sea. AOD time series of MRC and AERONET at Dakar, Capo Verde, Ragged Point and La Parguera sites are presented in Figure 3.

Site	CAMSRA	MERRA-2	NAAPS-RA	MRC	Rank of MRC
Banizoumbou	0.13 | 0.17	0.10 | 0.10	0.11 | 0.13	0.10 | 0.11	~1 | 2
Capo Verde	0.07 | 0.07	0.06 | 0.05	0.06 | 0.07	0.06 | 0.06	~1 | 2
Dakar	0.07 | 0.11	0.07 | 0.07	0.08 | 0.10	0.06 | 0.08	1 | 2
La Laguna	0.06 | 0.05	0.06 | 0.05	0.06 | 0.05	0.05 | 0.04	1 | 1
Santa Cruz Tenerife	0.04 | 0.04	0.04 | 0.04	0.04 | 0.04	0.03 | 0.03	1 | 1
Ragged Point	0.05 | 0.03	0.03 | 0.03	0.03 | 0.03	0.04 | 0.03	3 | ~1
La Parguera	0.05 | 0.02	0.03 | 0.02	0.03 | 0.02	0.03 | 0.02	~1 | ~1
Guadeloupe	0.05 | 0.05	0.05 | 0.04	0.04 | 0.05	0.04 | 0.04	~1 | ~1
Key Biscayne	0.05 | 0.03	0.03 | 0.02	0.02 | 0.02	0.03 | 0.02	2 | ~1

1207   **Table 2.** Annual average Atlantic TC activity in the three seasons with the highest JJA

1208   Caribbean DAOD (2014, 2015 and 2018) and the three seasons with the lowest JJA Caribbean

1209   DAOD (2005, 2011 and 2017). Ratios between the three low and the three high DAOD seasons

1210   are also provided. Corresponding numbers for the Caribbean are provided in parentheses next to

1211   the total basin-wide numbers.

	Tropical Depressions and Named Storms	Named Storms	Hurricanes	Major Hurricanes	Accumulated Cyclone Energy
Three highest JJA Caribbean DAOD	12.3 (2.3)	11.3 (2.3)	6.0 (0.3)	2.0 (0.0)	86 (3)
Three lowest JJA Caribbean DAOD	23.0 (6.7)	21.3 (6.7)	10.7 (3.0)	5.7 (2.7)	199 (39)
Ratio	1.9 (2.9)	1.9 (3.0)	1.8 (9.0)	2.8 (N/A)	2.3 (13.0)

1212

1213

1214

Table 3. Correlation matrix between regionally-averaged multi-reanalysis-consensus (MRC) JJA tropical North Atlantic/Caribbean DAOD and 850 hPa U, 200 hPa U, 200 hPa minus 850 hPa U (zonal wind shear), 700 hPa RH, SST, Maximum Potential Intensity (MPI) and Genesis Potential Index (GPI) during JJA and ASO, respectively. Correlations that are statistically significant at the 90% level are highlighted in bold and those with asterisks are statistically significant at the 95% level. 850 hPa relative vorticity is not shown as none of these correlations were statistically significant.

Environmental Field	JJA tropical North Atlantic / JJA Caribbean	ASO tropical North Atlantic / ASO Caribbean
850 hPa U	**-0.63* / -0.79***	0.03 / **-0.66***
200 hPa U	0.34 **/ 0.81***	0.30 / **0.85***
200 minus 850 hPa U	0.43 **/ 0.83***	0.22 / **0.82***
700 hPa RH	-0.43 **/ -0.80***	-0.34 / **-0.55***
SST	**-0.71* / -0.75***	**-0.44** / **-0.79***
MPI	**-0.74* / -0.68***	**-0.47** / **-0.67***
GPI	**-0.75* / -0.76***	**-0.62* / -0.69***

1225 **Table 4.** Correlation matrix between JJA and ASO values of 850 hPa U, 200 hPa U, 200 minus
1226 850 hPa U, 700 hPa RH and SST over the tropical North Atlantic and the Caribbean,
1227 respectively. Correlations that are statistically significant at the 90% level are highlighted in
1228 bold, and those with asterisks are statistically significant at the 95% level.

Environmental Field	Tropical North Atlantic	Caribbean
850 hPa U	**0.51***	**0.84***
200 hPa U	**0.71***	**0.88***
200 minus 850 hPa U	**0.72***	**0.90***
700 hPa RH	**0.48**	**0.74***
SST	**0.77***	**0.85***

1229

1230

Table 5: Correlations of MRC JJA Caribbean DAOD or JJA tropical North Atlantic (TATL) DAOD with the JJA or ASO Oceanic Nino Index (ONI) and the AMM. Correlations that are statistically significant at the 90% level are highlighted in bold. Correlations that are statistically significant at the 95% level are marked with *.

	JJA Caribbean DAOD				JJA TATL DAOD			
	CAMSRA	MERRA-2	NAAPS-RA	MRC	CAMSRA	MERRA-2	NAAPS-RA	MRC
JJA ONI	0.33	0.29	**0.50**	**0.44**	0.24	0.18	0.28	0.26
ASO ONI	0.42	0.41	**0.61***	**0.54***	0.38	0.30	0.42	0.41
JJA AMM	**-0.72***	**-0.70***	**-0.63***	**-0.76***	**-0.58***	**-0.65***	-0.36	**-0.60***
ASO AMM	-0.42	**-0.45**	-0.30	**-0.45**	-0.33	**-0.52***	0.01	-0.33

Table 6. Partial correlation matrix between MRC JJA Caribbean and tropical North Atlantic (TATL) DAOD and annual Atlantic basin-wide ACE while controlling for ENSO (using the JJA ONI) and the AMM (using JJA AMM index). Linear correlations (without controlling for the climate modes) between DAOD and ACE, AMM and ENSO indices and ACE are also listed for comparison purposes. Correlations that are statistically significant at the 90% level are highlighted in bold, and those with asterisks are statistically significant at the 95% level. Note that the thresholds for statistical significance are different for partial correlation and linear correlation, as the degrees of freedom are different between the two.

	ACE (ctrl. for ENSO)	ACE (ctrl. for AMM)	ACE	ACE (ctrl. for Caribbean DAOD)	ACE (ctrl. for TATL DAOD)
MRC Caribbean DAOD	**-0.62***	-0.29	**-0.61***	-	-
MRC TATL DAOD	-0.39	-0.07	-0.41	-	-
AMM index (JJA/ASO)	-	-	**0.59*/0.45**	0.26/0.26	**0.48**/0.37
ONI (JJA/ASO)	-	-	-0.12/-0.20	0.20/0.18	-0.02/-0.05

1248

Figures:

1249

1250
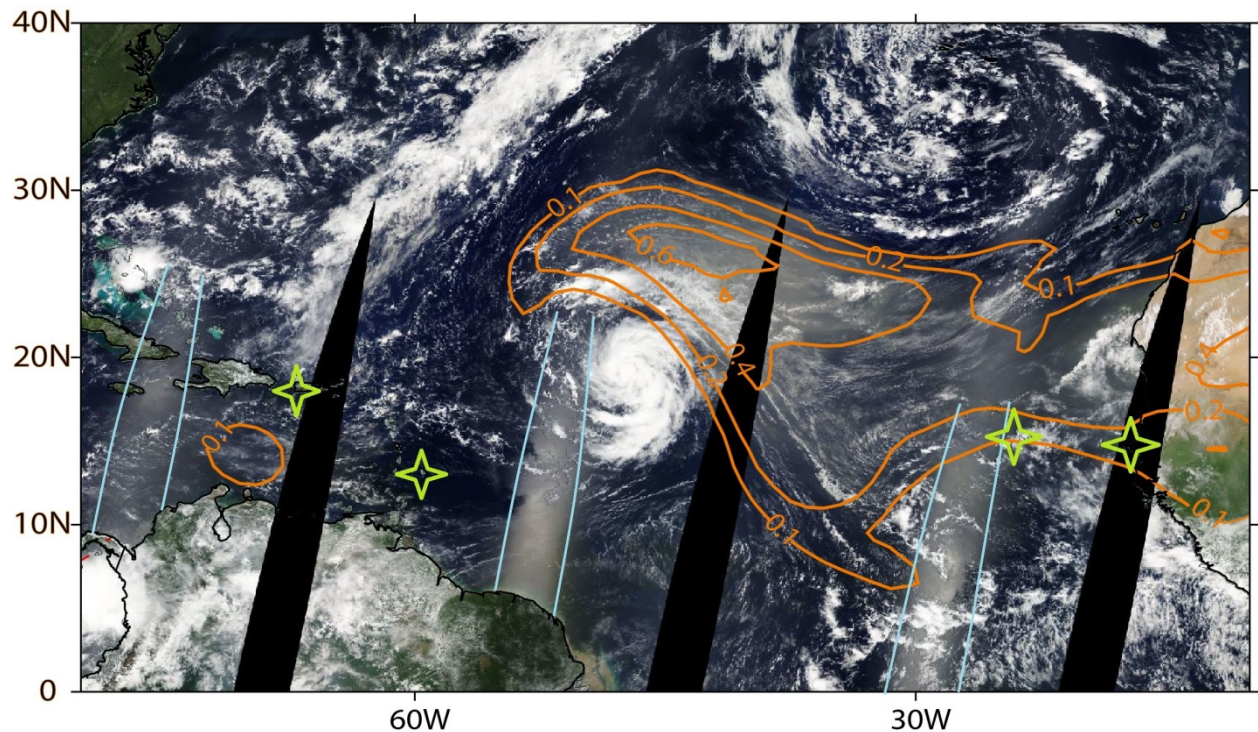
Figure 1. True-color Terra MODIS satellite imagery composited on 12 September 2012 and
overlaid with NAAPS-RA 550 nm dust aerosol optical depth (DAOD, an approximate measure
of total atmospheric column of dust aerosol mass, unitless) isopleths, showing Hurricane
Nadine's interaction with the SAL. Nadine is located in the middle of the image. African dust
appears as a light transparent brown haze in between the African coast and Nadine and wrapping
around the northern periphery of the storm. Note that areas of sunglint (narrow regions between
the light blue curves) are similar in color to the dust aerosols, but have the same orientation as
the satellite orbits and are located approximately mid-way between satellite coverage gaps (black
regions oriented south-southwest to north-northeast). Satellite imagery courtesy of the Moderate
Resolution Imaging Spectroradiometer (MODIS) flying on NASA's Terra satellite and available
from https://worldview.earthdata.nasa.gov/. The stars in light green represent four sites used for
validation purposes, including Dakar, Capo Verde, Ragged Point and La Parguera in order from
east to west.

1251
1252
1253
1254
1255
1256
1257
1258
1259
1260
1261
1262
1263

1264

1265

1266
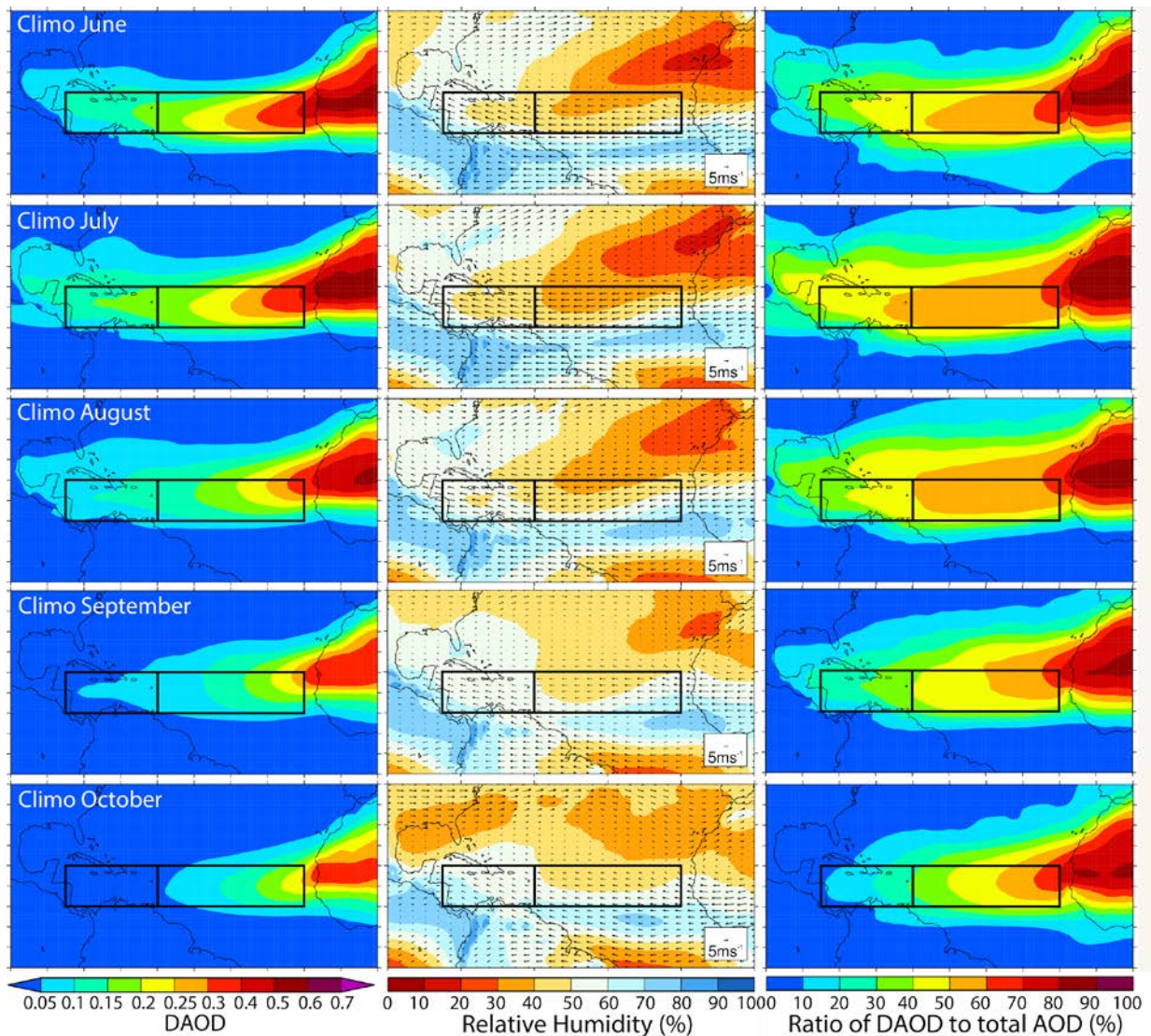
1267

Figure 2. Climatological (2003-2018 average) monthly mean DAOD (left column) and the ratio
of DAOD to total AOD (right column) for June-October based on the MRC. The middle column
shows the climatological 700 hPa RH (color shading) and horizontal wind vectors from ERA-
Interim. Black boxes denote the MDR, including the Caribbean (left, 10º-20ºN, 85º-60ºW) and
the tropical North Atlantic (right, 10º-20ºN, 60º-20ºW, denoted "TATL").

1273

1274
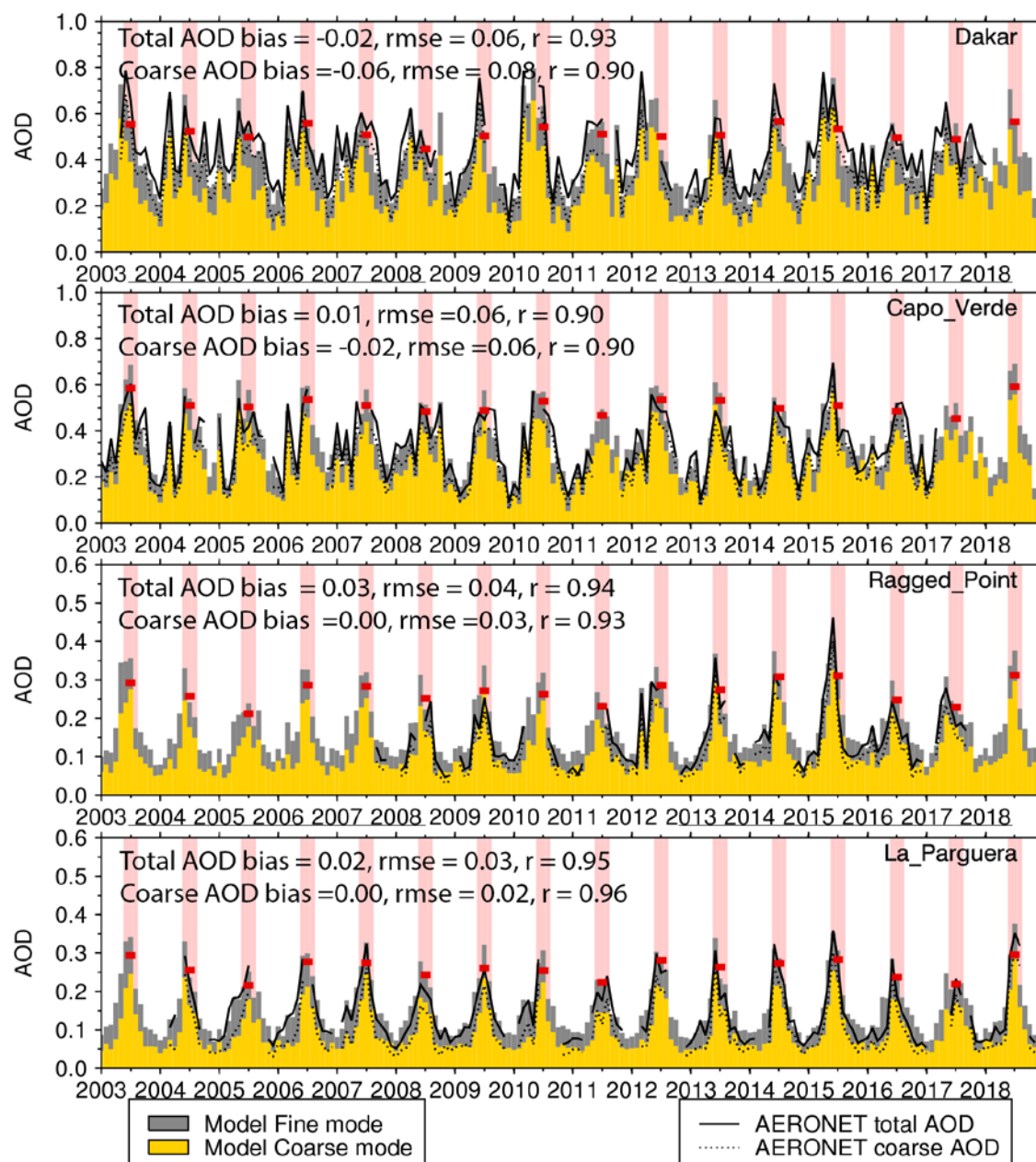
Figure 3. Monthly mean Version 3 L2 AERONET and MRC 550nm modal AODs at four
African dust-impacted sites: Dakar, Cape Verde, Ragged Point and La Parguera from east to
west. JJA are highlighted with pink shading ,and JJA seasonal average total AOD from MRC are
shown with red bars. Annotations for each time series show bias, RMSE and correlation (*r*) of
monthly averages calculated from the MRC.

1280

1281
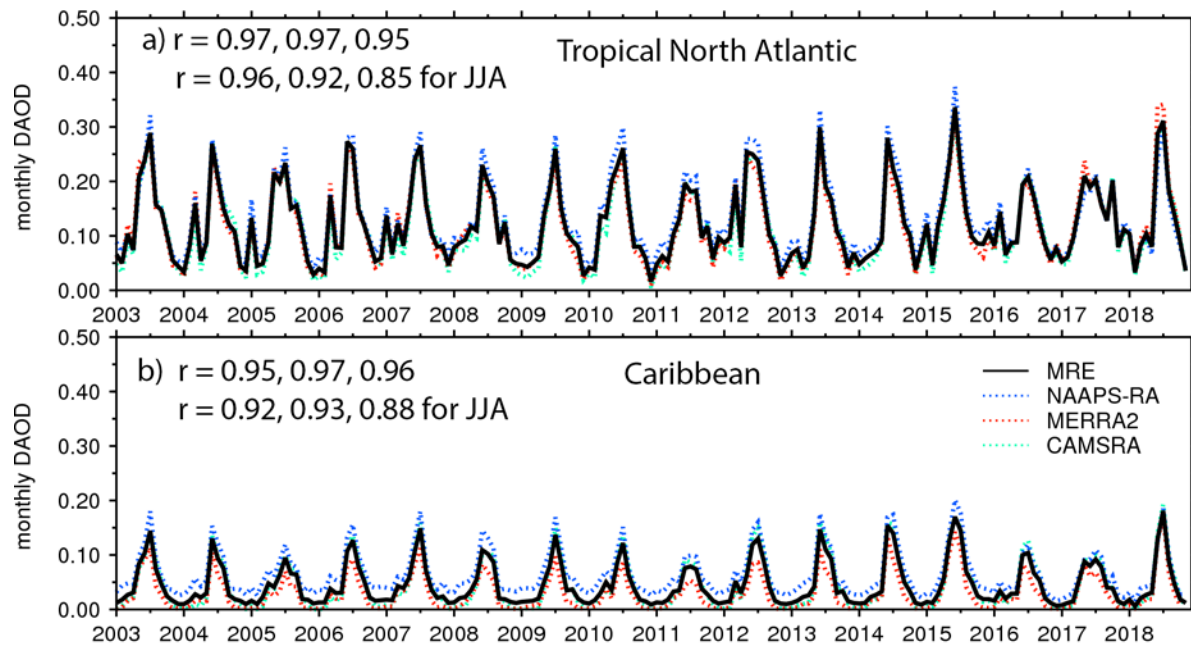
1282
1283 **Figure 4.** Monthly DAOD at 550nm from CAMSRA, MERRA-2, NAAPS-RA and MRC from
1284 2003-2018 for the (a) tropical North Atlantic and the (b) Caribbean. Correlations between
1285 CAMSRA and MERRA-2, CAMSRA and NAAPS-RA, MERRA-2 and NAAPS-RA are
1286 displayed in sequence for all months and for JJA-only respectively.
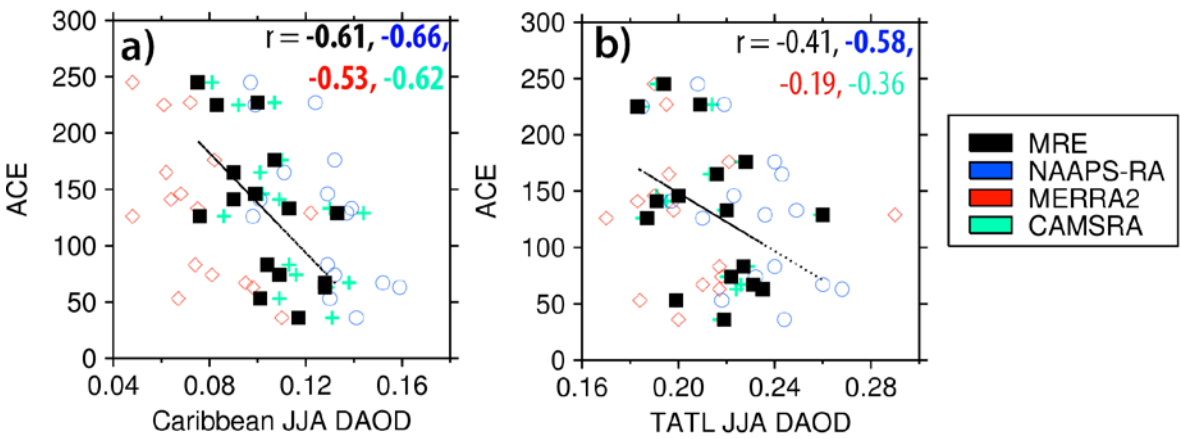
Figure 5. Scatterplot showing the relationship between annual Atlantic Accumulated Cyclone Energy (ACE) and JJA region-averaged DAOD from MRC, NAAPS-RA, MERRA-2 and CAMSRA over the (a) Caribbean and (b) the tropical North Atlantic. One unit of ACE equals 10^4 kt^2. Correlations (*r*) between ACE and DAOD are color-coded for different DAOD products and overlaid on each plot, and statistically significant correlations are in bold. The possible causes of the DAOD difference between the reanalysis products are discussed in Section 3.1.

1296
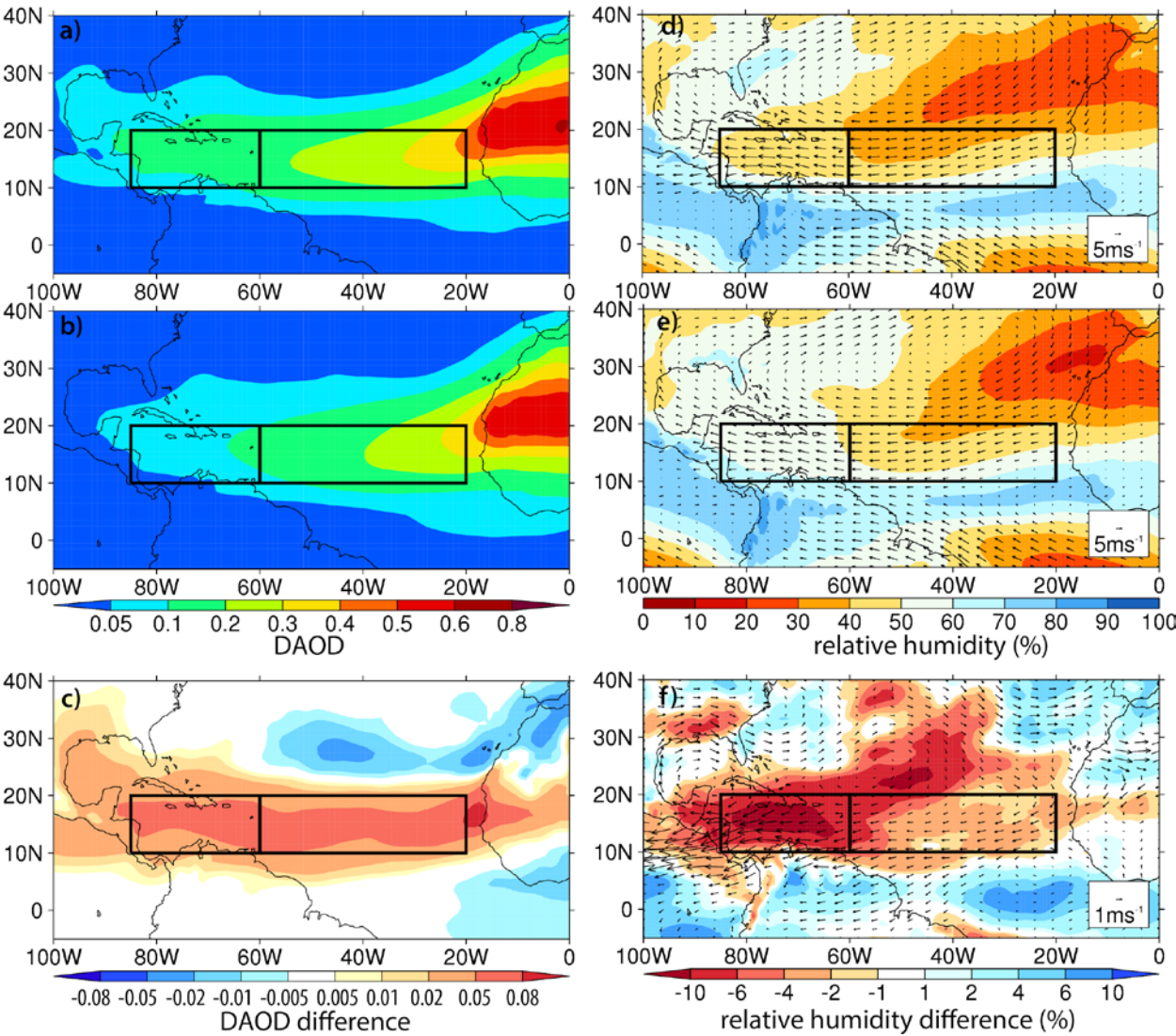
1297
1298 **Figure 6.** Left: MRC JJA composite of DAOD for the three Atlantic hurricane seasons from
1299 2003-2018 with (a) the highest JJA Caribbean DAOD (2014, 2015 and 2018), (b) the lowest JJA
1300 Caribbean DAOD (2005, 2011, and 2017), and (c) the difference between the two (highest minus
1301 lowest). Right: The corresponding JJA composite of 850 hPa wind (vectors) and 700 hPa RH
1302 (color shading).

1303

1304
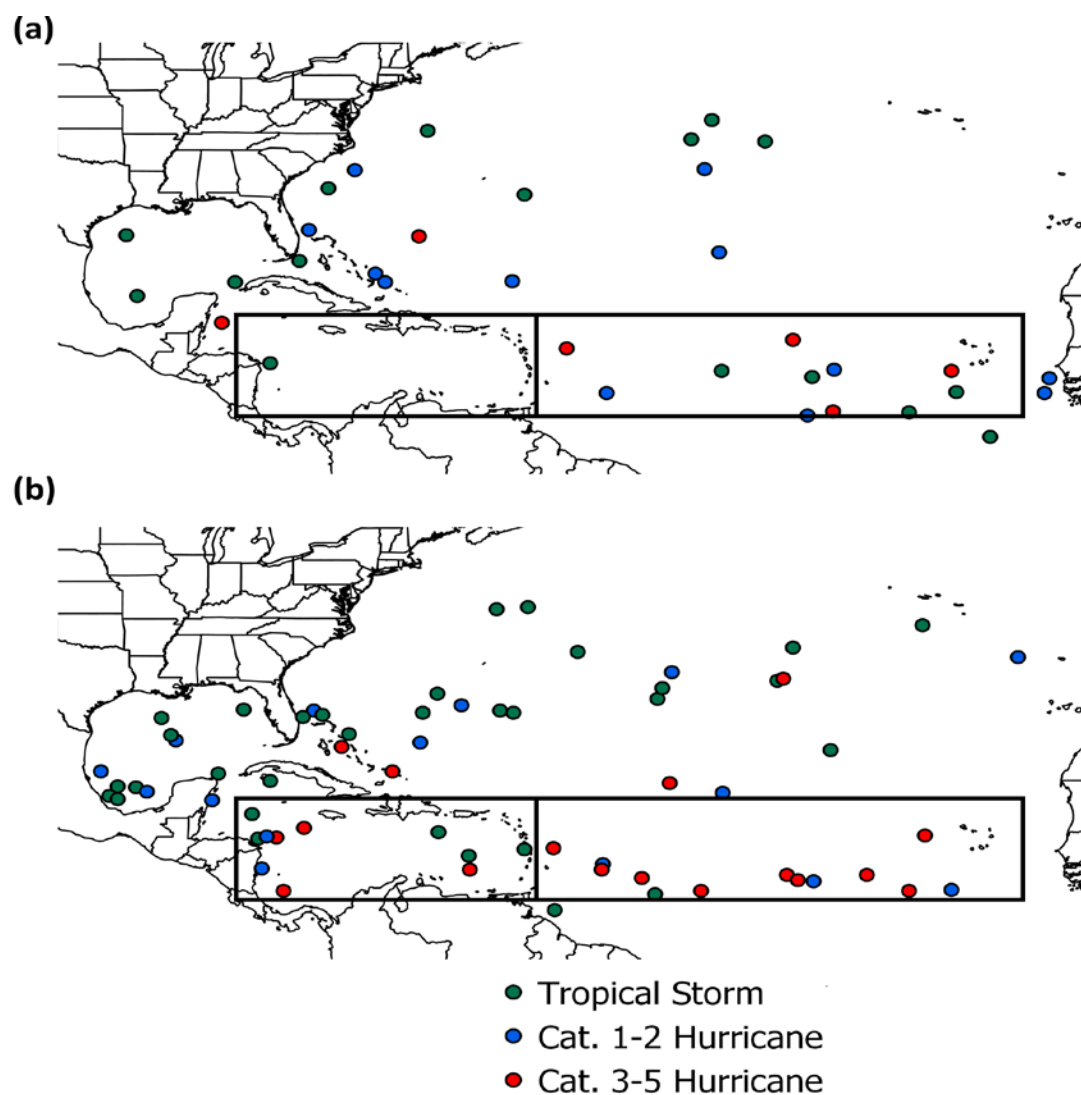
1305

1306

1307 **Figure 7.** Formation locations of Atlantic named storms during the three seasons with (a) the
1308 highest Caribbean JJA DAOD (2014, 2015 and 2018) and (b) the lowest Caribbean JJA DAOD
1309 (2005, 2011, and 2017). Also displayed are the maximum intensity that each TC reached.

1310
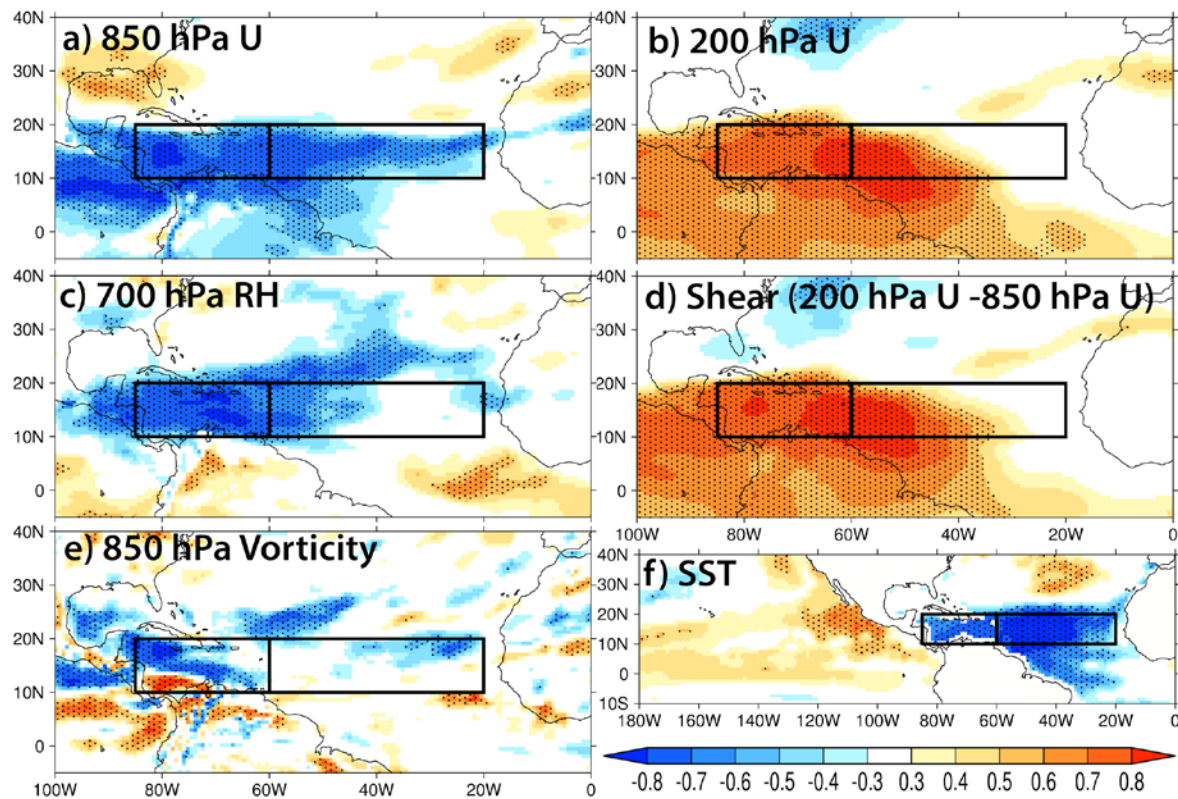
1311
1312 **Figure 8.** Correlation between MRC JJA regionally-averaged DAOD in the Caribbean and JJA
1313 (a) 850 hPa U, (b) 200 hPa U, (c) 700 hPa RH, (d) zonal wind shear, (e) 850 hPa relative
1314 vorticity and (f) SST. Correlations over the black dotted areas are statistically significant.

1315

1316
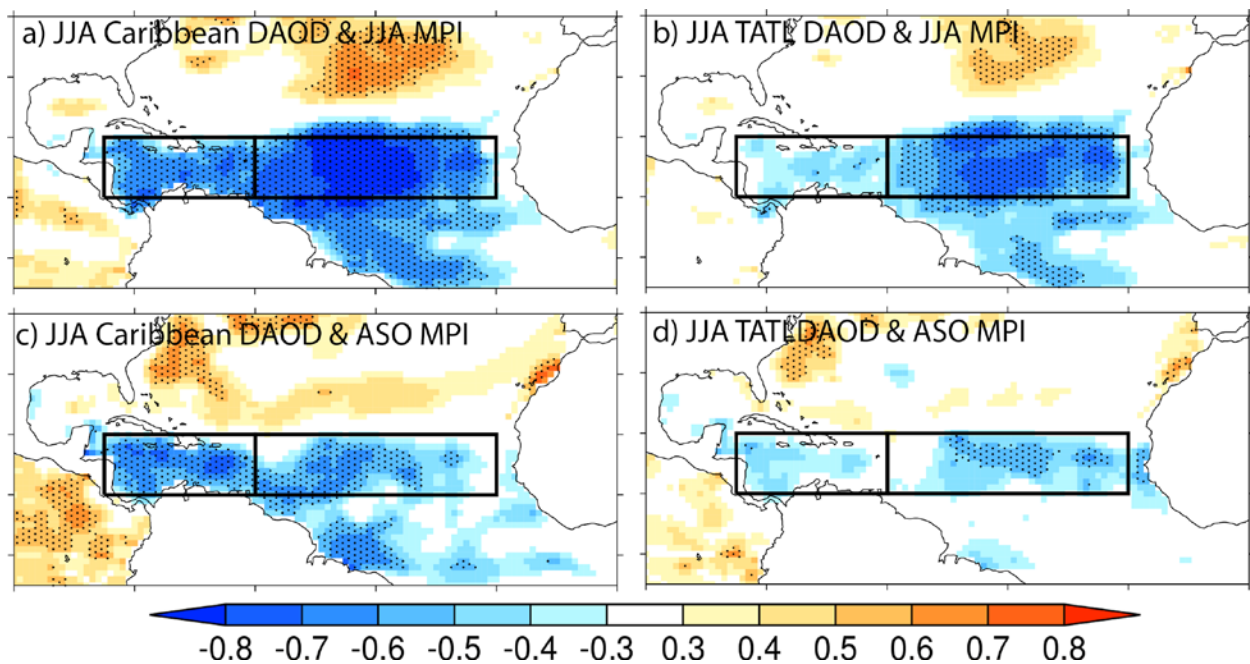
Figure 9. Correlation between (a) MRC JJA regionally-averaged DAOD in the Caribbean and JJA Maximum Potential Intensity (MPI), (b) MRC JJA regionally-averaged DAOD in the tropical North Atlantic (TATL) and JJA MPI, (c) JJA Caribbean DAOD and ASO MPI and (d) JJA TATL DAOD and ASO MPI. Correlations over the black dotted areas are statistically significant.

1323
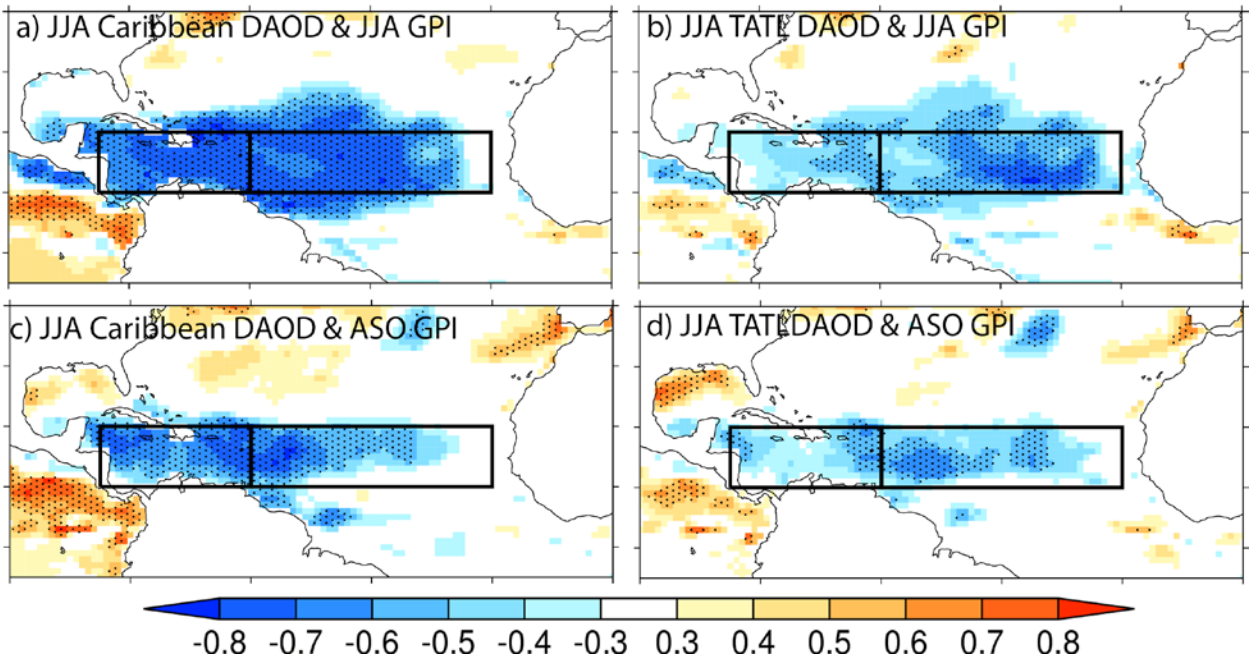
1324
1325 **Figure 10.** As in Fig. 9, but for the Genesis Potential Index (GPI).

1326

1327